

Review

Dielectric Elastomer Sensors with Advanced Designs and Their Applications

Holger Böse * and Johannes Ehrlich

Fraunhofer Institute for Silicate Research ISC, Neunerplatz 2, 97082 Würzburg, Germany;
johannes.ehrlich@isc.fraunhofer.de

* Correspondence: holger.bese@isc.fraunhofer.de

Abstract: Dielectric elastomer sensors (DESs) have been known as highly stretchable strain sensors for about two decades. They are composite films consisting of alternating dielectric and electrode layers. Their electrical capacitance between the electrodes is enhanced upon stretching. In this paper, a variety of advanced designs of DESs is introduced. An explanation of how these sensors work and how they perform in terms of capacitance versus deformation or load force is provided. Moreover, the paper describes how the sensor design affects the sensor characteristics in order to achieve a high measuring sensitivity. The most relevant quantities to be measured are distance variations or elongations, forces and pressure loads. It is demonstrated that the sensor design can be supported by Finite Element Method (FEM) simulations. In the second part of the paper, possible applications of the advanced DESs are outlined. Pure sensor applications to detect or monitor pressure or deformation are distinguished from other applications, where sensors form a part of a human–machine interface (HMI). DESs are predestined to be used in contact with the human body due to their softness and flexibility. In the case of an HMI, a dosed load on a sensor by the user’s hand enables the remote control of arbitrary technical functions. This can preferably be realized with an operating glove, which exhibits different categories of DESs. Possible applications of DESs are described with the support of functional demonstrators.

Keywords: capacitive sensors; dielectric elastomer; strain sensors; pressure sensors; sensor design; simulation; sensor applications; human–machine interfaces; operating glove



Citation: Böse, H.; Ehrlich, J. Dielectric Elastomer Sensors with Advanced Designs and Their Applications. *Actuators* **2023**, *12*, 115. <https://doi.org/10.3390/act12030115>

Academic Editor: Federico Carpi

Received: 28 December 2022

Revised: 16 February 2023

Accepted: 22 February 2023

Published: 8 March 2023



Copyright: © 2023 by the authors. Licensee MDPI, Basel, Switzerland. This article is an open access article distributed under the terms and conditions of the Creative Commons Attribution (CC BY) license (<https://creativecommons.org/licenses/by/4.0/>).

1. Introduction

Dielectric elastomers (DEs) are a class of smart materials that have attracted a lot of attention in the last two decades [1,2]. DEs are composite materials that consist of an elastomer film covered by electrode layers on both sides. Like elastomer film, the electrode layers must also be stretchable without losing their conductivity.

Principally, all elastomer materials can be used for the preparation of a simple layered composite structure. However, most studies have concentrated on two elastomer materials: acrylics and silicones. In the case of acrylics, a commercial material known as VHB 4910 and VHB 4905 from the company 3M has been widely used due to its softness, its extreme stretchability and its manageability in preparing a dielectric elastomer composite. This material is suitable for basic investigations but not for technical applications due to its pronounced viscoelasticity, which causes strong creep and relaxation effects in the stretched state [3].

In contrast, most silicone elastomers are relatively stable with respect to creep, and they are mainly used for real applications [4]. The thin dielectric film between the electrode layers can be prepared with liquid precursors, which are chemically crosslinked to the elastomer network by thermal treatment. Depending on the crosslinking density, the hardness and Young’s modulus of the elastomer can vary within a wide range. The Young’s modulus has a significant influence on the performance of DEs in various applications.

Another important material parameter is permittivity, which can be enhanced by the introduction of particles with high permittivity to the silicone elastomer [5] or the chemical modification of the polymer chains with electrically polarizable molecular groups [6–8].

For the electrode layers on both sides of the elastomer film, conductive particles adhered to the elastomer film or compounded to a gel or an elastomer composite are mainly used. The most common compositions consist of carbon-based nanoparticles such as carbon black, graphite, graphene or carbon nanotubes in a silicone matrix [9]. The compositions are used to achieve a higher conductivity of the electrode material. Additionally, metal particles, such as silver-coated copper flakes, are also used [10]. In all cases, the particle concentration in the matrix must be above the percolation threshold to achieve the required conductivity. Moreover, the interparticle contacts and the resulting conductivity must remain even when the elastomer film is stretched.

When an electric field is applied between two electrodes, they attract each other using electrostatic forces. This attraction leads to a thickness compression of the soft elastomer film. Additionally, the elastomer film expands in its area dimensions due to the volume incompressibility of elastomer materials. The deformations of the elastomer composite in terms of thickness reduction and area expansion are the exploitable effects of dielectric elastomer actuators (DEAs). Most investigations on dielectric elastomers deal with their actuation capabilities. Different designs of DEAs have been studied and reported in the literature [11–16]. Generally, strong electric fields with field strengths of some 10 kV/mm are required to generate significant deformations of DEAs, which need high voltages of 1 kV or more. Attractive applications of dielectric elastomer actuators were identified as controllable valves [17,18], pumps [19], loudspeakers [20], optical lenses with a tunable focus [21,22] and other optical components [23], robotic grippers [24] and other actuation elements of soft robots [25], as well as human–machine interfaces with haptic feedback [26].

Another field in which dielectric elastomers can be applied is converting mechanical to electrical energy [27–30]. Such dielectric elastomer generators (DEGs) operate in a circular process. In this process, the dielectric elastomer film is stretched by external forces. Thereafter, the elastomer film with the two electrode layers, which is a deformable capacitor, is charged with an external voltage source. In the following step, by removing the external force, the elastomer film relaxes, thereby lifting the electrical charges on the capacitor to a higher energy level. This is equivalent to converting a part of the mechanical deformation energy to electrical energy. In order to achieve acceptable efficiency, the DEG has to be operated in the same high-voltage regime as the DEA. Possible applications of DEGs are the extraction of large energy quantities from wind or water motions, such as sea waves [31], as well as harvesting small energy quantities in shoes from walking motion [32].

Besides DEAs and DEGs, the third exploitation field addressed by dielectric elastomers is the sensing of mechanical quantities [33,34]. Dielectric elastomer sensors (DESs) have also been an area of interest in recent years due to their simple operation and versatile applications. Since the dielectric elastomer composite is a deformable capacitor, it also works as a sensor that measures the deformations of objects by recording the change in their capacitance [35]. When the simple dielectric elastomer film strip is stretched in one dimension by an external force, its length is increased, thereby enhancing the area of the strip. Due to the constant volume of the elastomer, the thickness is decreased. Both dimensional changes contribute to the enhancement of the capacitance. This behavior leads to a simple strain sensor that covers a strain range of more than 100% due to the large stretchability of elastomer materials. Furthermore, with the known relation between stretch force and strain of the sensor film, the DES can also be used as a force sensor. It should be mentioned that DESs were already modified to measure non-mechanical quantities such as humidity and temperature [36], but this is beyond the focus of this paper, which only deals with electromechanical sensors. In review articles, various aspects of DESs are explained [36,37], whereas other reviews consider DESs together with DEAs [38,39].

In contrast to the exploitation of dielectric elastomers in DEAs and DEGs, DESs work at low voltage with a few volts since only measurements of the capacitance have to be

conducted. The low voltage allows safe operation without the risk of electrical breakdown, which can occur with DEAs and DEGs. Furthermore, common and inexpensive low-voltage electronics can be used for DESs. The capacitance may be measured with microprocessors, which are commercially available in large quantities at low costs.

DESs can be used in connection with corresponding DEAs, where the sensor monitors the deformation of the actuator. This may be achieved with the integration of the sensor film on the actuator with separated electrode layers for high and low voltage [40]. Alternatively, the same electrodes are used for actuation and sensing, where the low-voltage signal of the sensor must be separated from the high voltage of the actuator [41–44]. The latter operation mode of the DEA's self-sensing is a special exploitation of DESs with high importance since this double use of the dielectric elastomer enables the monitoring of the DEA actuation without the necessity of an additional sensor. According to this high relevance, a large number of publications deal with the self-sensing of DEAs [45–52].

In all exploitations of dielectric elastomers for actuation, energy conversion and sensing, the quality of the stretchable electrodes plays a significant role. According to this significance, some publications describe details of the procedures for manufacturing the electrodes. As an example, Fasolt et al. give an overview of the effect of screen-printing parameters on the sensor and actuator performance of dielectric elastomer membranes [53]. Araromi et al. present an approach for the production of dielectric elastomer layer composites with the application of laser ablation and oxygen plasma activation of the elastomer surfaces [54].

Besides self-sensing, DESs also exhibit a high potential for a multitude of applications apart from the combination with DEAs. DESs have properties that cannot be achieved with other kinds of strain and force sensors. Conventional mechanical sensors are mostly hard and almost not stretchable. An example of common sensors is given by strain gauges, which measure the change in the electrical resistance at strains of less than 1%. In contrast, dielectric elastomer sensor films can be stretched by more than 100% and are capable of measuring corresponding strains. Therefore, DESs are especially appropriate for applications in soft environments with high flexibility, large compliance and corresponding extended deformations. An example is the human body, which can move in complex patterns. Here, DESs allow the tracking of body motions in different degrees of freedom [55–58]. A very special application is the use of DESs in underwater environments, where the influence of water on the sensor capacitance must be carefully excluded [59]. Furthermore, DESs were already applied for human touch recognition [60]. Xu et al. describe an efficient multi-frequency method to detect the localization of applied finger pressure with reduced wire connections to the DES [61].

In recent years, various publications have appeared that describe the design of dielectric elastomer sensors, their characteristics and possible applications. Generally, it can be distinguished between different sensing modes, depending on the kind of mechanical load that acts on the sensor. These sensing modes comprise measurements of tension, pressure and shear loads, where the deformation and the corresponding force are related to each other by the sensor design and the stiffness of the sensor material.

The basic design of DESs, known since the research activities on dielectric elastomers began about 25 years ago, is that of the simple layered composite film consisting of the elastomer film with two electrode layers, which is used as a highly stretchable strain sensor. This DES film is the dominant dielectric elastomer sensor type, mostly used for various applications and is already commercially available [62–64]. Typical applications are the tracking of body motions, especially motions of fingers detected by sensors, which are integrated into a glove [65] or a wetsuit, for virtual reality (VR) environments [66]. Other technical applications of dielectric elastomer strain sensors concern the recording of machine motions, the detection of the radial expansion of polymer tubes by internal pressure [67], as well as the monitoring of civil structures such as bridges [68,69].

A special shape of dielectric elastomer sensors is a tubular one [70,71]. This design fits well with the pneumatic McKibben actuators with their cylindrical design, where the

tubular DES can be easily integrated. Accordingly, various papers describe the use of DESs in a McKibben actuator to monitor its actuation [72,73]. Another unusual design of DESs was proposed by Kofod et al., who developed a fiber with an elastic core surrounded by alternating electrode and dielectric layers. This fiber can be used as an actuator but also as a sensor, as the capacitance between the electrodes depends on the stretch of the fiber [74]. DESs can be exploited for the measurement of deformations or forces in more than one dimension as well. Girard et al. present a two-dimensional strain sensor for position feedback in human–machine interaction [75]. A six-axis capacitive force/torque sensor based on DESs was proposed by Kim et al. [76].

Not many approaches that describe sensor designs that significantly deviate from the simple basic design of a long strain sensor film with a dielectric and two electrode layers have been published [77–79]. The aspect ratio of the sensor film length and width in the simple basic design has been identified as an important impact on the capacitance increase upon stretching the strain sensor. When elongating the sensor film, the width becomes smaller, which reduces the capacitance increase. In order to make the sensor more sensitive, rigid sticks perpendicular to the sensor length were proposed, which reduce the narrowing of the sensor film upon its stretching [80]. Other approaches describe auxetic structures in the strain sensor, which also impede the disturbing constriction of the sensor film [81,82].

Besides the well-known dielectric elastomer strain sensors, capacitive elastomer sensors were also studied, which detect pressure loads or compression deformations of the sensor. The simple stretchable dielectric elastomer film used for strain measurements is not suitable for this task. If the sensor film is compressed between two flat and rigid surfaces, nearly no increase in the capacitance can be detected unless an extremely high pressure is applied because elastomer materials are principally volume-incompressible. This volume incompressibility is expressed by the Poisson figure of 0.5, which is common for elastomer materials and implies that the compression in thickness must lead to a corresponding expansion in area. However, friction between the elastomer film and the surrounding rigid surfaces generally hinders the area expansion. The high mechanical resistance against thickness compression can be reduced by the use of multi-layer stacks of alternating dielectric and electrode layers due to the bulging effects of the stack, which is equivalent to an area expansion in the middle of the multi-layer stack. A similar effect is caused by a thick elastic substrate under the pressure sensor if a hard object indents the sensor and deforms it locally [83].

A dielectric elastomer pressure sensor with high measuring sensitivity requires a volume-compressible structure. Some approaches for such DE pressure sensors have been described in the literature [84–93]. The volume compressibility is generally achieved by the integration of voids in the elastomer structure. One possible approach is the use of an elastomer foam or a porous structure of the elastomer, where the voids can be easily compressed [85–91]. Another possibility is the integration of defined hollow microstructures in the elastomer, which generate compressibility [92,93]. The planar arrangement of DE pressure sensors allows the realization of sensor arrays for locally resolved pressure monitoring [94–96].

Possible applications of dielectric elastomer pressure sensors have also been identified in connection with the human body, where hard sensors would restrict comfort. DE pressure sensors may be used to monitor the pressure acting on the foot when the person is walking or to record the pressure distribution of a sitting person on a seat. Another application concerns the measurement of gripping forces on the human hand.

Advanced dielectric elastomer pressure and strain sensors and their associated applications will be the main topic of this paper. The objective of the paper is to present a collection of new approaches for DESs with special designs for the sensitive measurement of pressure, force, compression or expansion. These special designs were introduced in recent years at various conferences “Smart Structures and Nondestructive Evaluation” within the section “Electroactive Polymer Actuators and Devices (EAPAD)” organized by the International Society for Optics and Photonics (SPIE). Based on these conference

contributions, the following sections of this paper give an overview of various designs of pressure and strain sensors, which demonstrate the versatility of DES technology. These advanced concepts show the extended potential of such dielectric elastomer sensors compared with the commonly known DE film strain sensors. The new DES designs focus on a high measuring sensitivity, which is expressed in the large relative increase in the measurable capacitance of the sensor upon loading. Related to the specific sensor design, the sensor characteristics will be described in detail. Moreover, the first approaches for finite element (FE) simulations of sensor properties will be given. Finally, possible applications of the advanced DES will be outlined in this paper.

2. Advanced Sensor Designs

For the benchmarking of the advanced DES, conventional dielectric elastomer strain sensor films serve as a reference. The most common DE strain sensor consists of an elastomer film covered by two electrode layers on both sides. The capacitance C is given by the simple equation

$$C = \epsilon_r \epsilon_0 \frac{A}{d} \quad (1)$$

where ϵ_r is the relative permittivity of the elastomer film, ϵ_0 is the absolute permittivity of vacuum, A is the area of the film and d is the distance between the electrodes. When the DES is stretched (see Figure 1), the capacitance between the electrodes is enhanced according to Equation (1). If the stretch occurs in the simple way shown in Figure 1, the capacitance should increase quadratically with the strain because the thickness of the elastomer film would decrease by the same factor as the length is increased due to the volume constancy of the elastomer material. However, in reality, the elastomer film transversally contracts when the film is stretched (see Figure 2). This contraction leads to a smaller than quadratic capacitance increase, which is nearly linear. It should be mentioned that a two-dimensional stretch of the DE film is also possible.

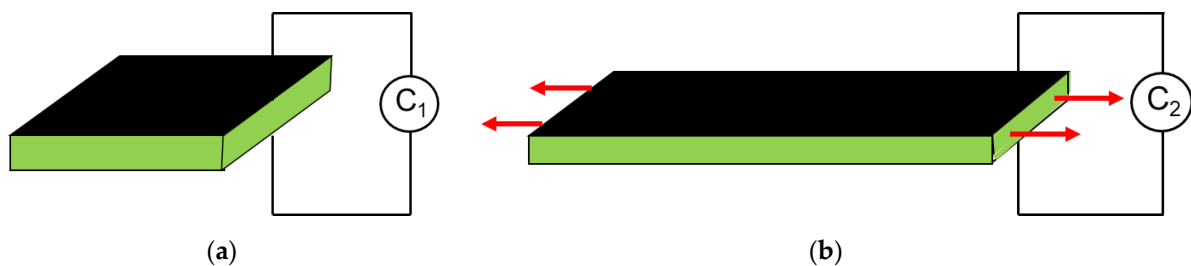


Figure 1. Scheme of a dielectric elastomer strain sensor (a) that is stretched in one dimension (b), where the capacitance is enhanced.



Figure 2. Scheme of a dielectric elastomer strain sensor (a) that is stretched with transversal contraction (b).

In a one-dimensional stretch, the strain sensor can also be used as a force sensor, which measures the stretch force by monitoring the capacitance increase. Here, the measuring sensitivity depends on the stretch stiffness of the sensor, which is determined by Young's modulus of the elastomer material and the width and thickness of the DE film.

In the manufacturing procedure of DESs, all elastomer materials can be principally used for the preparation of the two main components, the dielectric and the electrode

layers. To measure the sensor capacitance, electrical connections to a measuring unit are necessary. The electrodes usually consist of an elastomer matrix filled with conductive particles such as carbon or metal particles above the percolation threshold to enable the charging and discharging of the DE capacitor. The preferred elastomer material for the dielectrics and electrodes is silicone due to its high versatility of mechanical properties and easy processing. The hardness of the silicone elastomer can be tuned by the degree of the chemical crosslinking. Long polymer chains with a low density of crosslinks lead to a soft silicone elastomer, and short polymer chains with a high density of crosslinks lead to a hard elastomer. Strain sensors for the measurement of low stretch forces need a soft elastomer, but the softness is usually connected with a more pronounced viscoelastic behavior instead of nearly pure elasticity. For the manufacturing of thin films without or with conductive particles, liquid silicone precursors are processed with a blade-casting method, layer by layer, where the shape of the electrode layers is generated with a patterned mask.

As remarked before, the resulting flat DE films are sensitive to strain measurements, especially at high strains, but insensitive to pressure measurements between the surfaces of hard plates. The reason for this insensitivity is the volume-incompressibility of the elastomer, which restricts the thickness reduction upon pressure application. The necessary expansion in area is strongly hindered by the friction of the DES on the surfaces of the hard plates. When the applied pressure is reduced, the small area expansion is not fully reversible due to the same friction effect. This leads to a large hysteresis of the capacitance vs. pressure curve. Moreover, the achievable capacitance increase is very low due to the small deformation of the elastomer.

2.1. Advanced Pressure Sensors

As mentioned before, a moderate performance improvement of the pressure sensor between the hard plates can be achieved by stacking the sensor layers. The stacked DES consists of alternating elastomer layers as dielectrics and electrode layers. If the stack has a considerable thickness related to the area dimensions, the deformation pattern is different since the relatively thick elastomer sensor can bulge between the bottom and top plates to all sides in horizontal directions, which allows a moderate compression of the elastomer layers in thickness and an expansion in area. This mechanism is schematically depicted in Figure 3a.

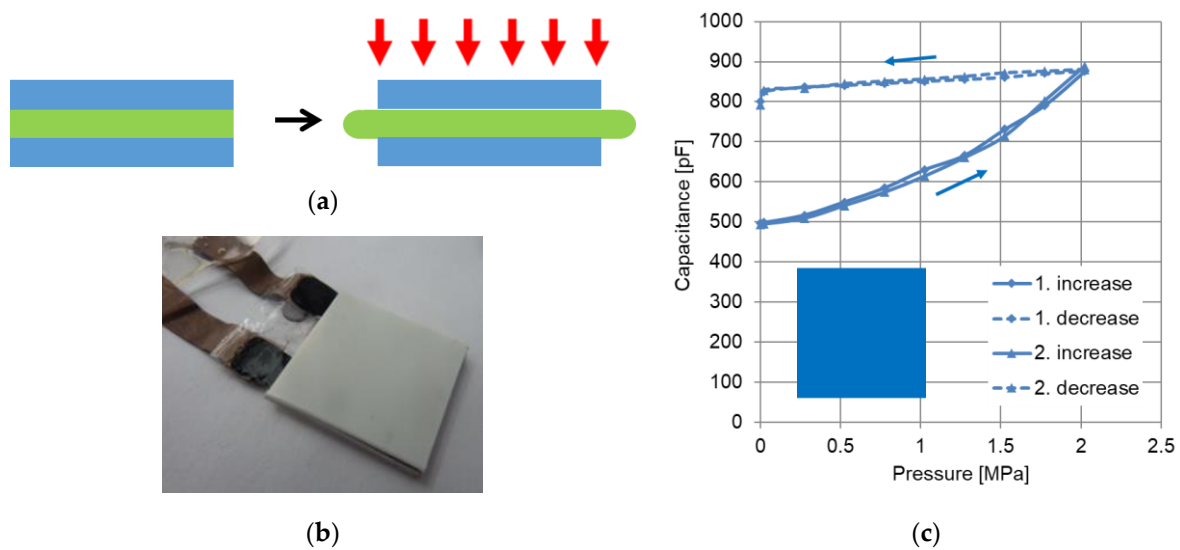


Figure 3. Scheme of the bulging of a dielectric elastomer pressure sensor with hard plates (a), photograph of the pressure sensor (b) and measured capacitance upon increase and decrease in pressure in two cycles (c) [97].

Figure 3b shows a photograph of such a sensor, which exhibits four dielectric layers, five electrode layers and two protective layers at the bottom and top with a total thickness of 630 μm . This multilayer film is covered by two rigid plastic plates with a thickness of 1 mm each. All layers except the plastic plates consist of silicone elastomer, where the electrode layers are filled with carbon black nanoparticles. In Figure 3c, the dependence of the measured capacitance on the applied pressure up to 2 MPa in two cycles of pressure increase and decrease is also represented. It is apparent that an extremely large hysteresis occurs due to the high friction between the deformable silicone part and the rigid hard plates. The large difference between the measured capacitance at increasing and decreasing pressure makes a reliable pressure determination with this sensor embodiment impossible.

A significant improvement can be achieved with modifications to the sensor design. The hard plastic plates are substituted by elastic silicone plates, which exhibit a pattern of openings distributed over the whole area [97]. Figure 4a reveals a scheme of the working mechanism, and Figure 4b shows a photograph of the modified pressure sensor. When high pressure is applied, the central part of the sensor (green in Figure 4a) can deform with bulging into the openings. This local bulging allows a stronger deformation and leads to a larger increase in the capacitance, thereby enhancing the measuring sensitivity. Moreover, the hysteresis between the capacitance at increasing and decreasing pressure is much smaller than that of the pressure sensor with hard plates without openings (see Figure 4c).

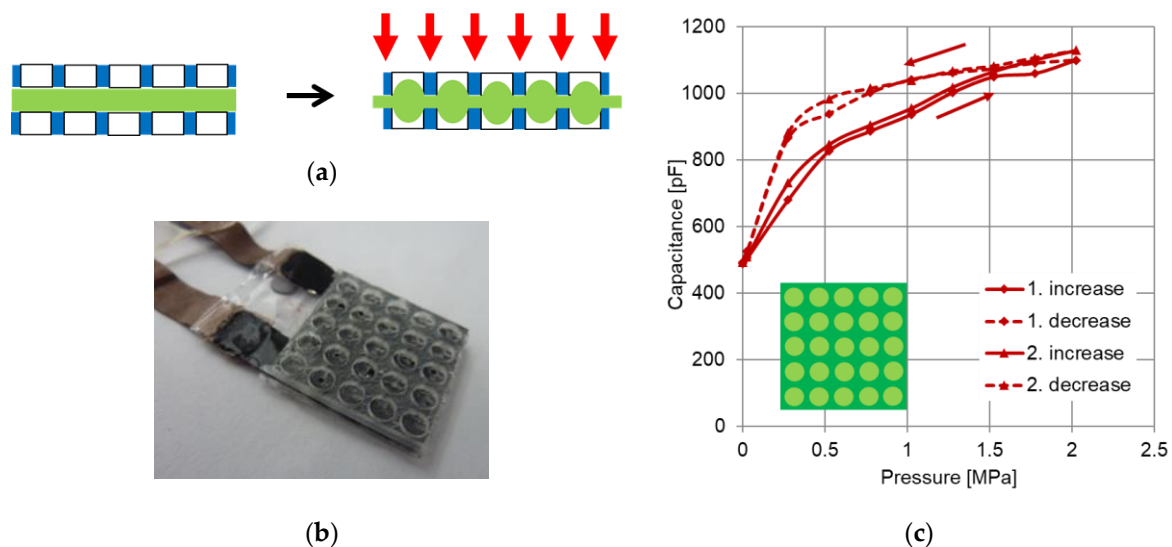


Figure 4. Scheme of the bulging of a dielectric elastomer pressure sensor with soft plates with openings (a), photograph of the pressure sensor (b) and measured capacitance upon increase and decrease in pressure in two cycles (c) [97].

The pressure sensor mechanism shown in Figure 4 is suitable for the measurement of relatively high pressure in the order of magnitude of 1 MPa. These sensors could be used for load monitoring in high-pressure applications such as bridge mounts, engine mounts and other elastomer dampers.

A strong enhancement of the sensitivity of dielectric elastomer pressure sensors is obtained with a sensor design that contains voids or pores in the elastomer structure. This partly hollow structure allows a compression already with low pressure without the necessity for the elastomer to expand into other directions. With this design, the dielectric elastomer sensor becomes volume-compressible, which allows a larger increase in capacitance [98,99].

Figure 5 depicts such a sensor with enhanced sensitivity. It consists of two parallel elastomer films with profiled inner surfaces and a flat elastomer film between the profiles [99]. The topographies of the two wave-shaped profiles are complementary, i.e., the

elevations of one profile fit into the depressions of the other profile. When the sandwich structure of the three films is compressed, the intermediate film designed as a strain DES is stretched. This sensor design converts a pressure load into a stretch load. The capacitance between the electrodes of the intermediate DES film increases with rising pressure. The DES film exhibits three electrode layers, where the two outer layers are set to electric ground potential in order to shield the inner measuring electrode from disturbing signals from the outside.

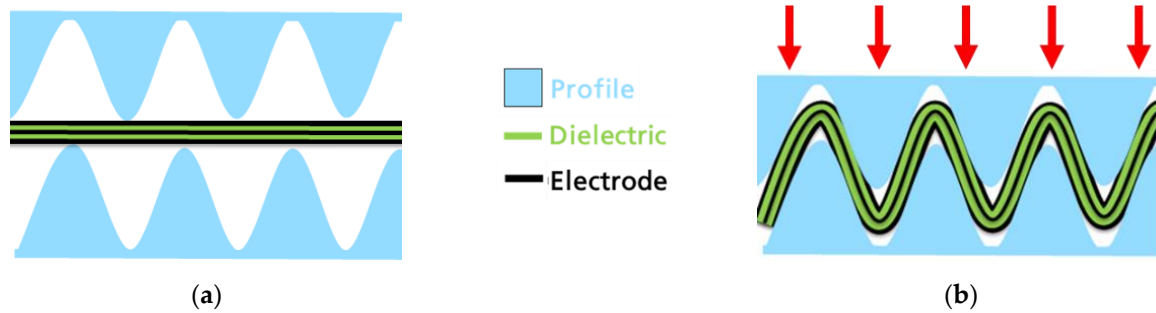
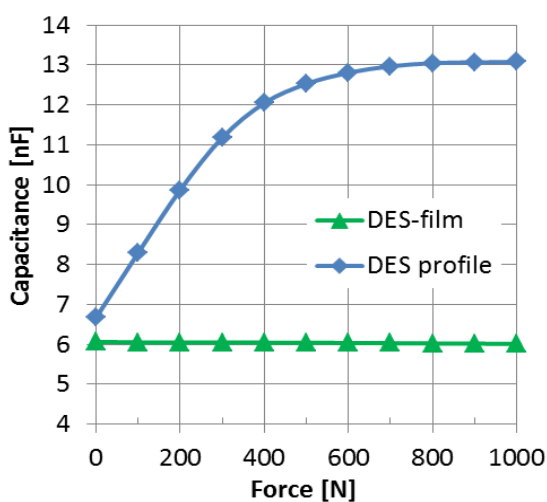


Figure 5. Scheme of a dielectric elastomer pressure sensor with two outer films with wave-shaped profiles and a flat dielectric elastomer strain sensor film with three electrode layers between the profiles in the unloaded state (a) and in the loaded state (b) [99].

Figure 6 reveals the dependence of the measured capacitance on the applied compression force and a photograph of a pressure sensor with wave profiles and with an area of $100 \text{ mm} \times 100 \text{ mm}$. The applied maximum force of 1000 N corresponds to a pressure of 10 N/cm^2 or 0.1 MPa. At a force of 400 N corresponding to a pressure of 0.04 MPa, the capacitance is nearly doubled. This demonstrates the high sensitivity of this sensor design compared with the former design shown in Figure 4, which is suitable for high-pressure measurements [99]. In addition to the graph of the sensor with wave profiles, the green line in Figure 6a also depicts the pressure dependence of the capacitance of a pure DES film, which is compressed between hard plates. It is obvious that this pure DES film with high sensitivity for strain measurements is not capable of detecting any pressure.



(a)



(b)

Figure 6. Dependence of the measured capacitance of a sensor with wave profiles and an intermediate DES film on the applied compression force compared with the corresponding curve of a pure DES film (a) and photograph of the sensor with wave profiles with an area of $100 \text{ mm} \times 100 \text{ mm}$ (b) [99].

The pressure sensor with wave profiles can be modified to another version, which is schematically shown in Figure 7. This sensor design with the wave profiles and the intermediate elastomer film is very similar to that in Figure 5. Only the ground electrodes in the intermediate film are shifted to the wave profile surfaces. However, this small modification has a strong impact on the sensor characteristics [99]. In the uncompressed state, the electrode layers are located at a quite large distance from each other, which leads to a small initial capacitance. With rising compression, the electrodes approach each other, thereby increasing the capacitance.

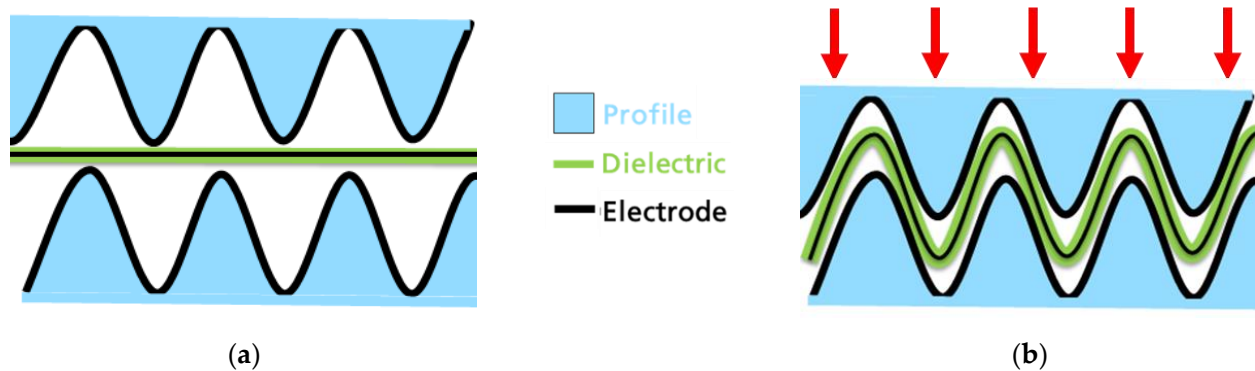


Figure 7. Scheme of a dielectric elastomer pressure sensor with two outer films with wave-shaped profiles and electrode layers on the profiles and an elastomer film with only one electrode layer covered by two dielectric layers between the profiles in the unloaded state (a) and in the loaded state (b) [99].

Figure 8a reveals the capacitance dependence of the modified sensor with the ground electrodes on the wave profile surfaces on the applied pressure. For comparison, the graph of the unmodified sensor with all three electrodes in the intermediate film is included in the same diagram. The curve of the modified sensor starts at a much lower capacitance level than that of the unmodified sensor, whereas both curves end at nearly the same capacitance, which can be explained by the full compression of the sensors, where the complementary profiles fit completely into each other and press onto the intermediate film from both sides. Due to the small initial capacitance, the modified pressure sensor exhibits an increase in the capacitance by a factor of about 21 at 0.1 MPa pressure. The capacitance increase is boosted by the displacement of the air in the voids since the permittivity of the dielectrics between the electrodes is progressively determined by the higher permittivity of silicone elastomer of the intermediate film compared with that of air, thereby enhancing the effective permittivity. These results demonstrate that the measuring sensitivity of the profiled pressure sensors with voids between the elastomer films is orders of magnitude higher than that of the pressure sensor shown in Figure 4. Figure 8b depicts photographs of the wave profiles with and without electrode coating.

Besides the wave profiles, a large variety of other profile shapes is possible for the design of pressure sensors. The shape of the profile determines the sensor characteristics in terms of capacitance versus compression force. Instead of wave profiles, elastomer profiles with a pattern of parallel rectangular bars can be used as well [99]. Figure 9 depicts the scheme of a pressure sensor with two elastomer sheets carrying a two-dimensional array of knots covered by electrode layers and an intermediate third elastomer film with the third electrode between the profiles.

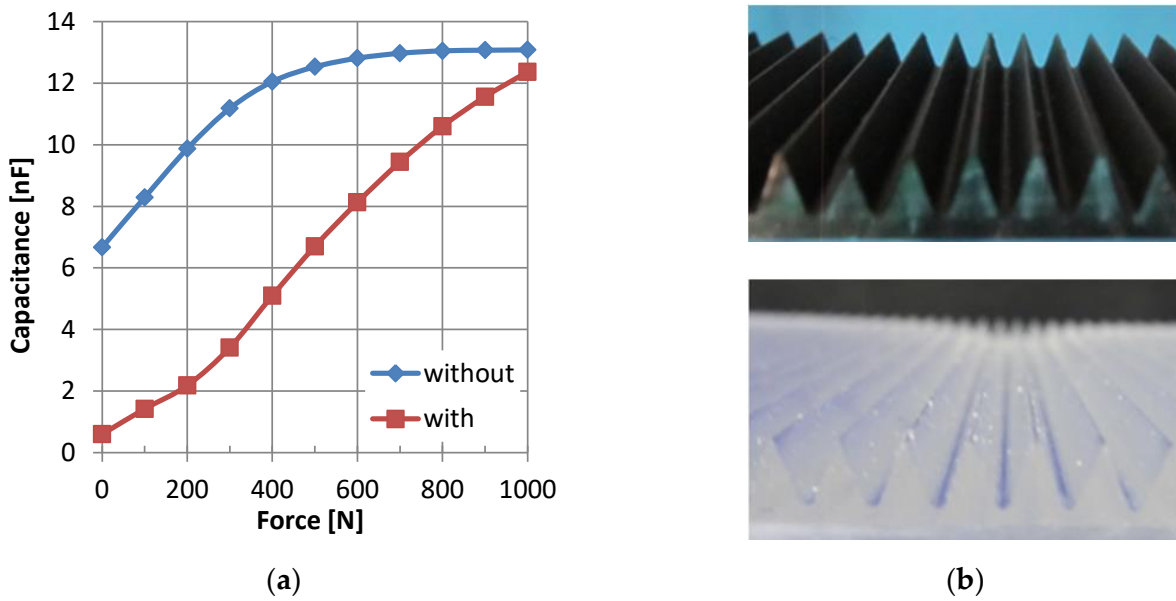


Figure 8. Dependence of the measured capacitance of a sensor with wave profiles covered by electrode layers (with in legend) on the applied compression force compared with the corresponding curve of a sensor without electrode layers on the wave profiles (without in legend) (the sensor area is 100 mm × 100 mm) (a) and photographs of a wave profile with electrode layer (top) and a wave profile without electrode layer (bottom) (b) [98].



Figure 9. Scheme of a dielectric elastomer pressure sensor with two knot-shaped profiled outer films with electrode layers and an elastomer film with only one electrode layer covered by two dielectric layers between the profiles in the unloaded state (a) and in the loaded state (b) [99].

As with the wave-shaped profiles, the three electrode layers approach each other when the sensor is compressed. However, the stretch of the intermediate film causes an increase in the capacitance only in the first phase of the compression until the knots of one profile press the intermediate film against the other profile. In the second phase of the compression, the knots and the intermediate film are squeezed, thereby diminishing the distance between the electrodes, which results in a further enhancement of the capacitance.

Figure 10a shows two elastomer sheets with knot profiles. The upper one is not covered, and the lower one is covered by an electrode layer. Furthermore, Figure 10b depicts the comparison of the characteristics of pressure sensors with different profile shapes, e.g., wave profiles, bar profiles and knot profiles, where all profiles are covered by electrode layers [100]. The knot profile sensor reaches a smaller final capacitance at the highest pressure of 0.1 MPa than the sensor with wave profiles, but the initial capacitance is also lower. The result is a slightly smaller increase factor of 16 at 0.1 Mpa compared with the factor 21 of the wave profile sensor, but in the low-pressure region, the sensitivity of the knot profile sensor is higher due to the steeper increase in the capacitance. It can be concluded that the design principle of dielectric elastomer pressure sensors offers a large variety of different sensor characteristics, where the shape of the capacitance vs. pressure curve can be tuned by the profile shape.

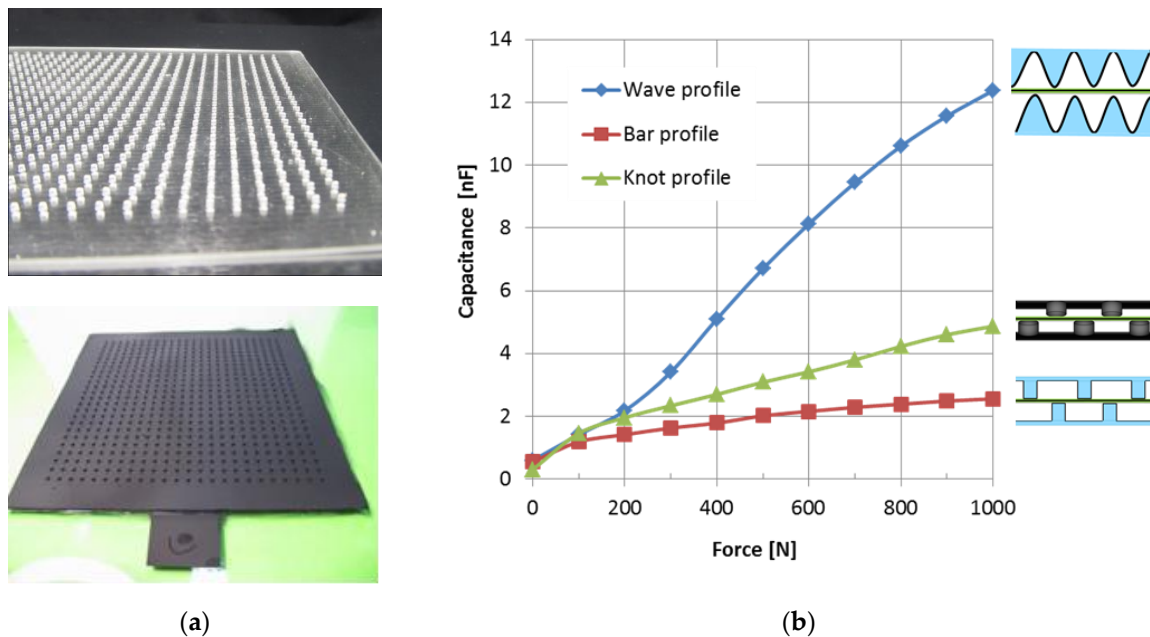


Figure 10. Photographs of elastomer sheets with knot profiles without and with electrode layer (a) and comparison of the dependence of the measured capacitance of pressure sensors with wave profiles, bar profiles and knot profiles on the applied force, where all profiles with an area of $100 \text{ mm} \times 100 \text{ mm}$ are covered by electrode layers (b) [100].

Another set of parameters with an impact on the sensor characteristics arises from the material properties, which play an important role as well. As an example, the hardness or stiffness of the intermediate film in the sensor between the wave profiles affects the sensor characteristics strongly. An elastomer film with a high Shore hardness requires a higher-pressure load on the sensor to be stretched with the same strain as an elastomer film with a lower hardness. The same effect has a larger thickness of the intermediate film, but thicker dielectric layers on the intermediate film reduce the final capacitance at complete compression of the sensor and, therefore, the possible available range of the capacitance increase. Furthermore, the permittivity of the dielectric elastomer can also influence the measuring sensitivity of the pressure sensor. In the unloaded state of the sensor with voids, the permittivity of the dielectric is an effective value between the higher permittivity of the elastomer and the lower permittivity of air. When the sensor is compressed, the air is removed, which gives an increasing dominance of the elastomer permittivity, leading to a strong enhancement of the capacitance.

Finally, a further impact on the sensor characteristics comes from the location of the electrode layers in the sensor, as has been demonstrated with the example of the pressure sensors with wave profiles. If the electrode layers have a large distance in the unloaded state corresponding to a low capacitance and approach each other to a small distance upon loading, a strong enhancement of the capacitance results, which corresponds to a huge increase in the capacitance and a corresponding high measuring sensitivity.

For the manufacturing of silicone-based pressure sensors, the intermediate flat elastomer film with dielectric and electrode layers is prepared in the same way as strain sensor films. The other sensor components, such as the elastomer films with openings or with profiles, are processed by pouring the liquid silicone precursors into a suitably shaped molding tool, where the liquid silicone is chemically crosslinked in a thermal process to the elastomer film with the corresponding shape. If electrode layers have to be deposited on the profiled elastomer film, they are prepared with a spraying process. Finally, the different silicone films are assembled into the pressure sensor through a gluing process with liquid silicone, and the electrode layers are equipped with electrical connections.

2.2. Advanced Strain Sensors

Strain sensors are the original type of dielectric elastomer sensors, as shown before. The conventional design with two or more electrode layers separated by elastomer layers as dielectrics is very simple. The basic DES consists of only one dielectric center and two electrode layers (see Figure 1), which can be extended by further dielectric and electrode layers. Only a few modifications of this design have been reported. These sensors are capable of measuring large strains of up to 100% and more with high accuracy, which is about two orders of magnitude above the range of conventional strain gauges consisting of metal strips, whose electrical resistance is changed when they are deformed.

With DE strain sensors, the elongation can be measured over very large distances, depending on the length of the sensor. However, the measurement of low strains of about 1% or less over long distances is not very accurate due to the small increase in the capacitance and the corresponding low sensitivity. As a rule of thumb, 1% strain gives about a 1% increase in capacitance. For an enhancement of the strain measuring sensitivity, a modified design of the DE strain sensor can be used.

The advanced DE strain sensor consists of two zones, a short stretchable active zone and a long non-stretchable passive zone [101]. The measurable capacitance of the sensor is concentrated in the stretchable active zone, whereas the non-stretchable passive zone does not contribute to the capacitance. Figure 11 schematically depicts the design of this advanced strain sensor in comparison with a conventional strain sensor with three electrode layers. Photographs of conventional and advanced strain sensors are also revealed in Figure 11.

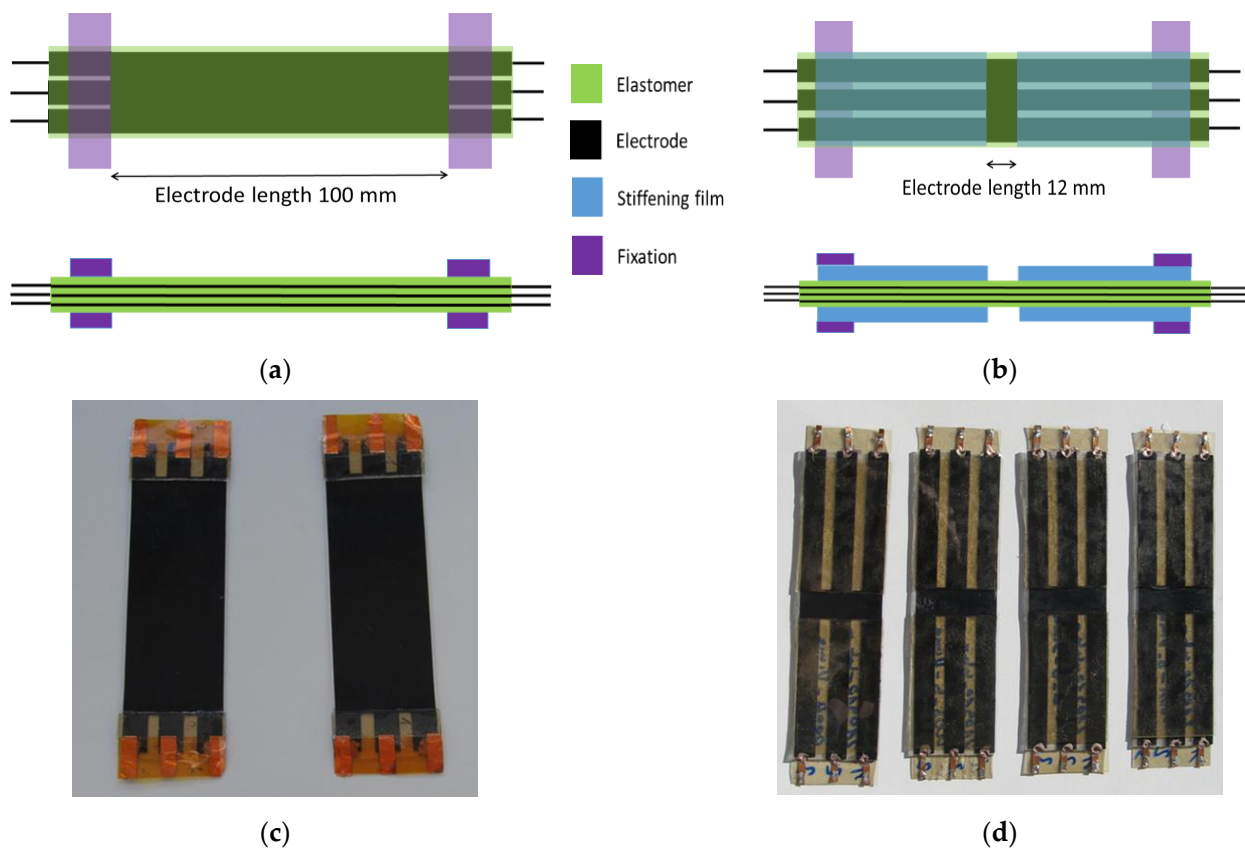


Figure 11. Scheme of a conventional DE strain sensor with two dielectric layers, three electrode layers and two outer protective layers in top view and in side view (a), scheme of an advanced DE strain sensor with the same layers in the center zone and two stiffening elements at both ends in top view and in side view (b) and photographs of conventional (c) and advanced strain sensors (d) [101].

When the whole sensor is stretched, the strain only occurs in the short active zone. The result is a relatively large strain in the active zone, but a small strain of the sensor related to the complete sensor length. This leads to a large relative enhancement of the capacitance increase due to the large local strain in the active zone. The factor of enhancement of the capacitance increase is given by the ratio of the total sensor length to the length of the active stretchable zone. The difference in the capacitance increase upon strain for the two sensor types is represented in Figure 12 for the limited strain range of the advanced sensor of 12%, corresponding to an elongation of 12 mm. However, a side effect is the resulting larger tension force of the advanced sensor at the same strain compared with the tension force of the conventional sensor with stretchability over its whole length.

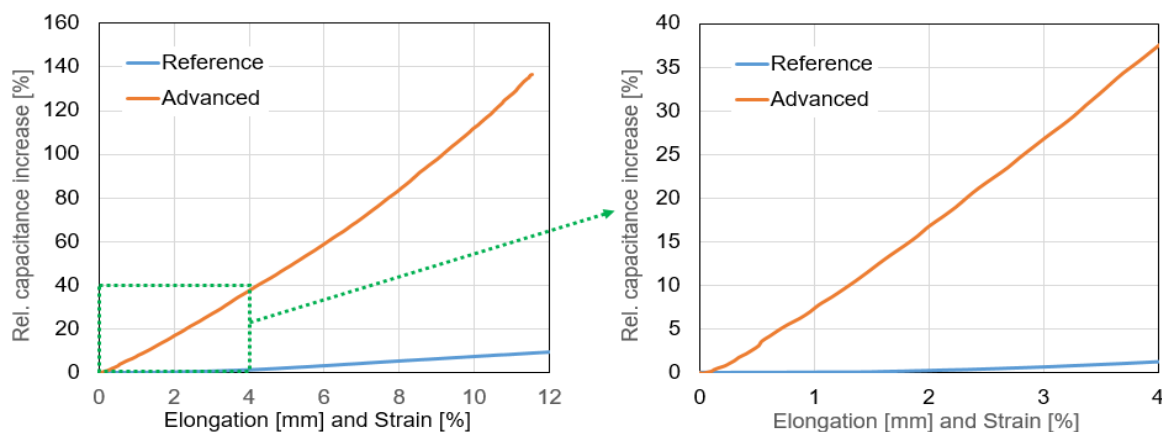


Figure 12. Comparison of the relative capacitance increase in the advanced strain sensor upon strain with that of the conventional strain sensor as reference [101].

The advanced strain sensor with enhanced measuring sensitivity can be advantageously used in applications, in which low strains at high stretch forces over long distances have to be measured. Examples of this scenario are identified in the monitoring of civil structures, such as bridges, large buildings and industrial facilities, where small deformations in the large structure have to be detected before strong or even fatal damages occur (structural health monitoring). Another example concerns the recording of periodic or cyclic motions with small amplitudes in mechanical devices such as dampers and shock absorbers in vehicles and machines.

Another type of strain sensor is characterized by an out-of-plane deformation of the DE film [102]. Here, the elastomer film with a preferably circular shape is clamped along its rim in a rigid frame. As known from other DE strain sensors, the sensor film has two or three electrode layers, whereas, in the case of three electrode layers, the outer electrodes shield the inner electrode. When a pressure load is applied on one side of the sensor film, the film bulges to the other side. As a result, the DE film is radially stretched, and the capacitance is enhanced.

A possible application of this sensor principle is the measurement of the pressure of gases and liquids. The capacitance increase is a measure of the pressure difference between the two sides of the sensor film. This kind of strain sensor can be exploited to monitor the filling level, such as, for instance, the water level in washing machines or dishwashers or for the measurement of the liquid level in a tank. A specific advantage of this sensor type is its extremely simple design, which enables a correspondingly easy manufacturing process of the sensor.

Figure 13 depicts the principle of measuring the hydrostatic pressure of a liquid in a vertical tube with the out-of-plane strain sensor at the bottom of the tube. Without liquid in the tube, the sensor is not deformed. However, when a liquid exerts hydrostatic pressure in the tube, the sensor bulges, the elastomer film is stretched and the capacitance is increased. Figure 13 also reveals a photograph of an out-of-plane sensor in a rigid frame.

The experimental evaluation of this sensor in a tube with different filling levels of water gave the results shown in Figure 14. The capacitance increases nearly linearly with the hydrostatic pressure, and the reproducibility is very high. The graph of the first cycle of water level increase and decrease is completely hidden by the second cycle. As silicone elastomer was used for the sensor film, almost no hysteresis between the increase and decrease in the water pressure was detected (see Figure 14a). Figure 14b depicts only a low creep of the capacitance over a time period of 60 min at the maximum hydrostatic pressure load on the sensor.

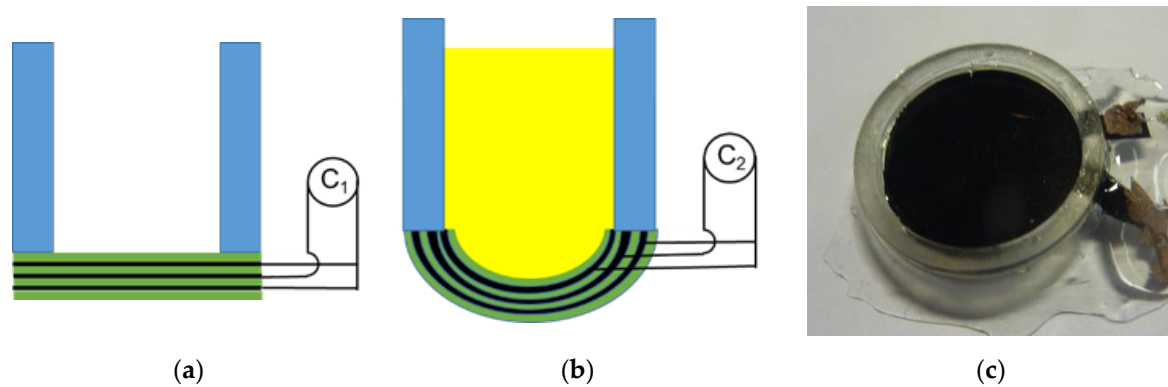


Figure 13. Out-of-plane DE strain sensor with two dielectric layers, three electrode layers and two outer protective layers at the bottom of a tube in a schematical representation in side view in the unloaded state (a) and in a loaded state with liquid pressure in the tube (b) and as a photograph (c) [102].

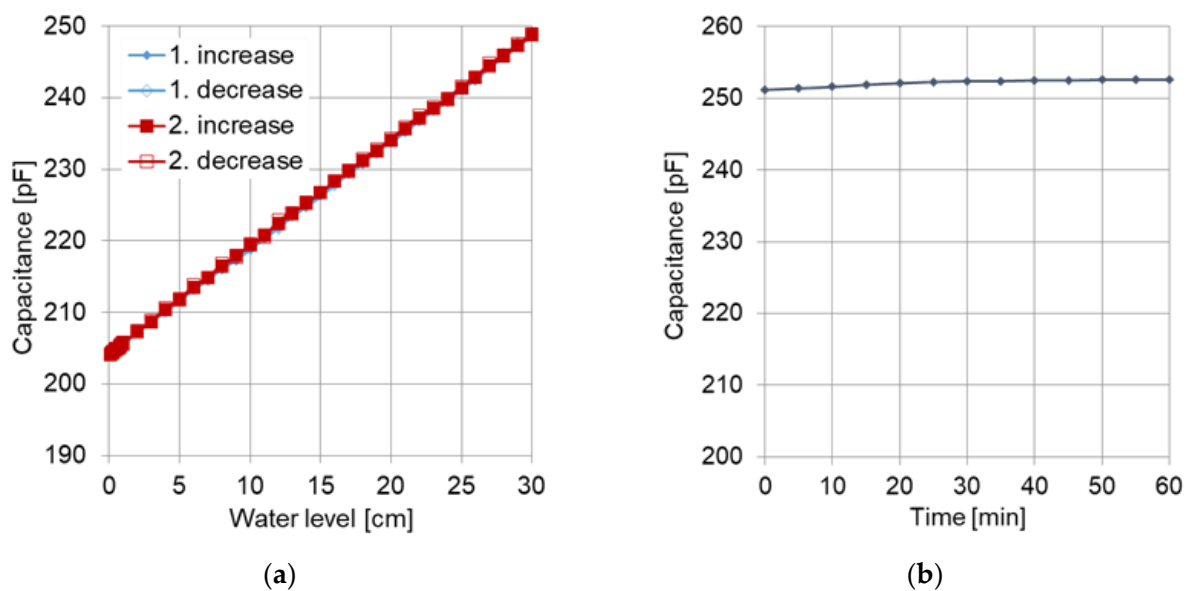


Figure 14. Measured capacitance of an out-of-plane DE strain sensor upon increase and decrease in the water level in the tube above the sensor in two cycles (a) and measured capacitance at 30 cm water level in the tube over 60 min (b) [102].

2.3. Simulation of Advanced Sensors

The deformation behavior of dielectric elastomer sensors under mechanical loading can be simulated with finite element methods (FEMs). Such simulations support the development of a special design of the sensor with defined properties. With the simulations, relevant sensor properties, such as the relation between the sensor deformation and the applied force or pressure, as well as the dependence of the capacitance on the deformation,

can be calculated. For the description of the elastic behavior of the elastomer, which is mostly silicone elastomer, linear elasticity models and nonlinear models can be used. Nonlinear models are preferred, if large deformations with high strain occur.

Two examples of FEM simulations on dielectric elastomer sensors are described in the following. They refer to the high-pressure sensor and to the strain sensor with enhanced measuring sensitivity, both of which have been represented before. The simulations were performed with the software COMSOL Multiphysics. They concern mechanical as well as electrical properties of the sensor, such as the elastomer deformation or the stretch force and the capacitance.

The first example refers to the high-pressure sensors with the multilayer dielectric elastomer film between two plates shown in Figures 3 and 4 [97]. In the first version, the plates are hard and flat (see Figure 3), and in the second version, the sensor exhibits elastic silicone plates with a pattern of openings (see Figure 4). The results of the FEM simulation in comparison with experimental data are depicted in Figure 15. In the first version, with hard plates without openings, the simulated initial capacitance at zero pressure and the final capacitance at 2 MPa fit well with the measured data, but between these limits, the simulated capacitance is slightly higher. For the sensor with softer silicone plates with openings, the simulated capacitance in the uncompressed state also fits the experimental data well, but with rising pressure, the simulated capacitance exhibits a lower increase.

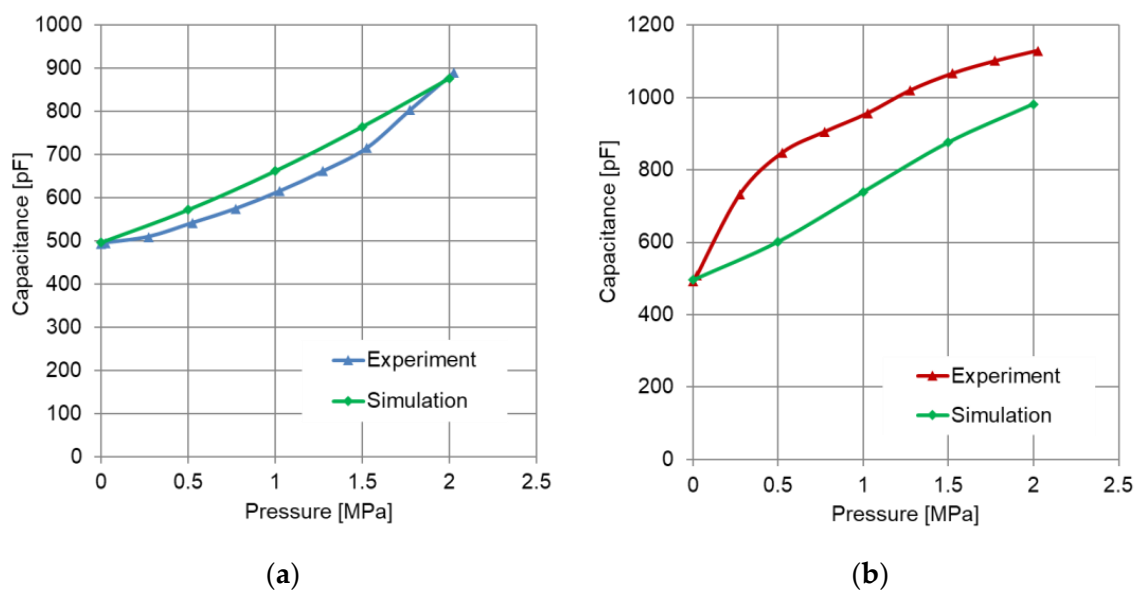


Figure 15. Comparison of the dependence of the capacitance of dielectric elastomer high-pressure sensors on the applied pressure received from experimental data and FEM simulations: sensor with hard flat plates (a) and sensor with elastic silicone plates with openings (b) [97].

Figure 16 reveals the calculated deformation of the high-pressure sensor with the soft silicone plates with openings in the compressed state. The intermediate multilayer DES film is squeezed and expands into the openings of the silicone plates, which is visible in the magnified representation in Figure 16b. Such a kind of deformation is not possible with a pure DES film loaded between hard surfaces without openings. The local bulging effect of the multilayer DES film explains the higher sensitivity of the high-pressure sensor with the silicone plates with openings. Here, the multilayer DES film can be more extensively compressed between the plates in all the area regions between the openings, which leads to a larger increase in capacitance. The compression of the sensor at 2 MPa pressure amounts to 460 μm , which is much larger than the corresponding compression of 180 μm of the reference sensor with hard plates without openings. However, the main benefit of the high-pressure sensor with the silicone plates with openings is the smaller hysteresis between

the capacitance curves at increasing and decreasing pressure. The hysteresis could not be simulated because friction, as an interface process with a complicated mechanism, plays a dominant role in the compression and relaxation of the sensor.

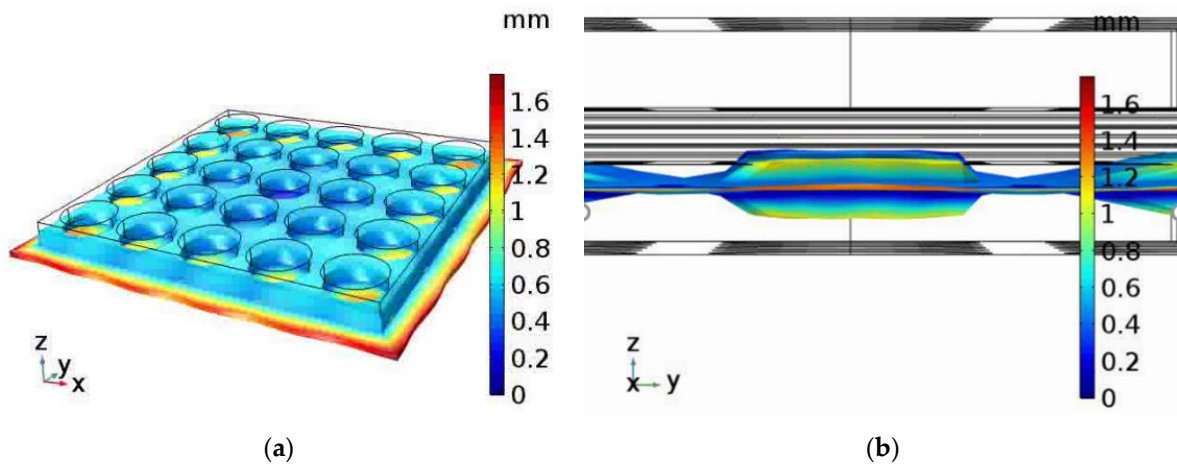


Figure 16. Calculated deformation of the sensor with elastic silicone plates with openings (a) and magnified side view of the bulging effect of the dielectric elastomer between two openings (b) [97].

The second example of the use of FEM simulation for dielectric elastomer sensors concerns the advanced strain sensor with enhanced measuring sensitivity caused by a long stiffened passive zone (see Figure 11) [101]. Figure 17 reveals the dependence of the simulated capacitance on the elongation for both sensors, the conventional DE strain sensor as the reference and the advanced strain sensor with the stiffened passive zone. The results of the simulation are compared with experimental data.

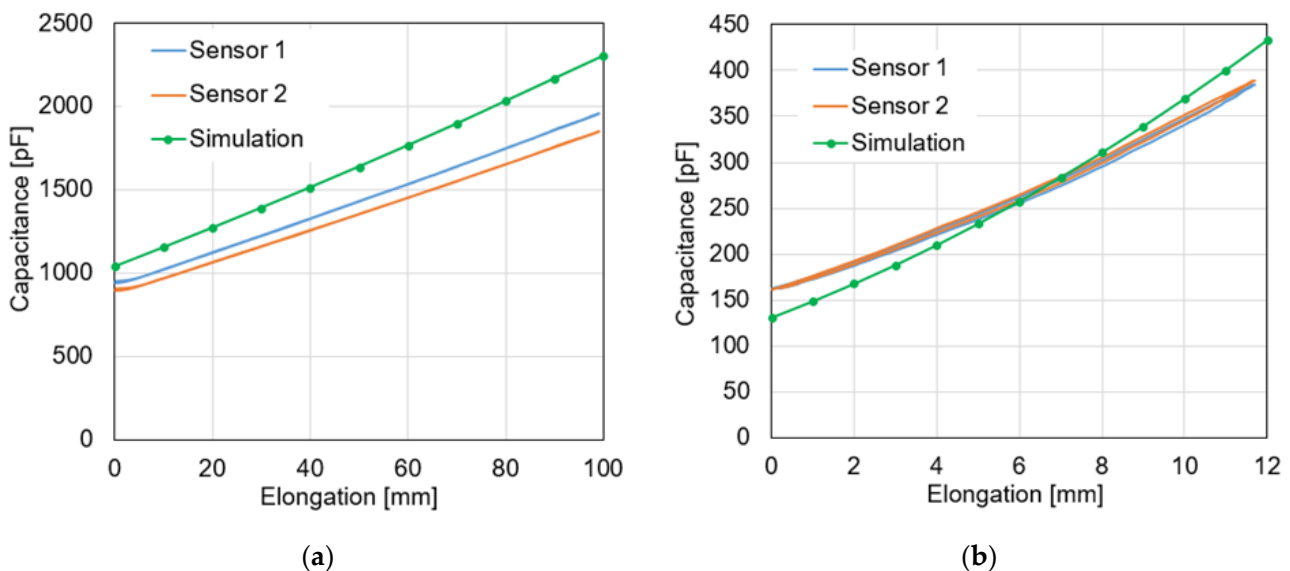


Figure 17. Dependence of the capacitance on the elongation from FEM simulation and from measurements on two sensors: conventional strain sensor as reference (a) and advanced strain sensor (b) [101].

In the case of the reference sensor, the calculated increase in capacitance with the elongation is nearly linear. The measured capacitance on two sensors also rises linearly but with a smaller slope than calculated, giving a higher deviation with large elongation. The linear dependence is typical for strain sensors with a large aspect ratio of length and width of the elastomer strip, which causes a strong transversal contraction when the sensor is

stretched. For the advanced strain sensor with the stiffened passive zone, relatively good agreement between experimental and simulated data was achieved. However, the curve of capacitance vs. elongation is nonlinear. This can be referred to as the small aspect ratio of the stretchable sensor zone, which is much less than 1, i.e., the length of the stretchable sensor zone is smaller than its width. The small aspect ratio prevents the strong transversal contraction of the elastomer strip and leads to a larger linear increase in capacitance when the sensor is stretched.

From the two examples of FEM simulation and a comparison with experimental data, it is concluded that the simulation can predict the sensor characteristics quite well. Therefore, FEM simulations on dielectric elastomer sensors are a valuable tool for the optimization of the sensor design and the properties in terms of the dependence of the sensor capacitance on the applied pressure in the case of a pressure sensor or on the elongation of a strain sensor, respectively.

3. Applications of Advanced Dielectric Elastomer Sensors

3.1. Sensor Applications

Some possible applications of advanced DESs were already mentioned in the preceding chapter, where they were related to the sensor design. The advanced sensors and their already referred possible applications comprise:

- Pressure sensors with an elevated pressure range for bridge mounts, engine mounts and other elastomer dampers;
- Strain sensors with an enhanced measuring sensitivity for structural health monitoring of civil infrastructure such as bridges, large buildings as well as industrial facilities;
- Out-of-plane strain sensors for recording the filling level of liquid-containing systems such as tanks, containers, washing machines, dishwashers, etc.

In the following section, various other applications of advanced DESs, for which the sensor performance was evaluated, supported by the construction and characterization of simple demonstrators, will be presented and discussed [100]. Soft capacitive elastomer sensors are especially advantageous in applications where the sensors are in close contact with the human body. Here, the inherent softness, flexibility and stretchability of DESs are required to avoid any inconvenience to the person wearing the sensors or being in contact with them.

A first example with high importance is the measurement of pressure, which a person sitting on a seat exerts on the seat surface and which reversibly is exerted on the person. Monitoring the pressure distribution over the seat surface with several sensors or with a regular two-dimensional sensor array is useful for operation in automotive seats to detect the actual position of the car passengers on the seats. With this information, the operation of the airbags could be controlled in order to select the most convenient execution in case of a crash.

Another sensible application of dielectric elastomer pressure sensors is in office chairs to monitor the attitude of the sitting person and the frequency and strength of his or her body movements. The monitoring and analysis of the sensor signals can support a healthier sitting over an entire working day. Figure 18 shows the demonstration of a cushion on a chair, which is equipped with four pressure sensors integrated into the cushion. The sensor capacitance data is wirelessly transmitted to a tablet computer, which displays a graphical representation of the body weight distribution on the chair. The size of the red circular areas on the screen indicates the pressure acting on the corresponding region of the cushion.



Figure 18. DE pressure sensor for seat applications (a) and demonstration of monitoring the weight distribution of a person on a chair cushion with four sensors (b) [100].

Similarly, a wheelchair user or an immobile person in a bed may be better protected against bedsores by monitoring pressure peaks of the body. With this information from the sensor system, the critical load in the identified body region can be selectively reduced.

In other applications, DESs can be worn on the human body. Besides monitoring foot pressure distribution in shoes, a corresponding benefit also exists in the detection of the pressure exerted by a knee prosthesis on an amputee who could be seriously affected by an arising decubitus. Figure 19 depicts an experiment where a dielectric elastomer pressure sensor was attached to the liner of a knee prosthesis. The sensor could detect the applied load of the prosthesis on the liner with high measuring sensitivity, which demonstrates the potential of the sensor technology.



Figure 19. DE pressure sensor attached on the liner of a knee prosthesis for an experimental evaluation [100].

Another application field with high importance is the monitoring of forces on the human hand when the hand grabs or holds an object. The same force and corresponding pressure are exerted by the hand on the object. The knowledge of this force may be relevant for protecting the health of a worker or for protecting fragile objects to be handled manually. For this purpose, soft and flexible dielectric elastomer sensors can be integrated into a glove to measure the bending movements of individual fingers with strain sensors and the contact forces on the fingers with pressure sensors when grabbing or holding an object.

Figure 20 reveals a demonstrator of a glove, which is equipped with a total of seven pressure sensors, five of which are located on the fingers and the other two on the palm. When the person wearing the glove grabs different objects, the pressure distribution on the various hand partitions is monitored by the DES and is represented as colored bars on a display. Of course, the measured load distribution depends on the shape and weight of the grabbed object. A corresponding approach may be used for the detection of the distribution of the applied pressure in a robotic gripping tool when it grabs an object. With this information, the gripping process can be controlled in order to protect fragile objects.

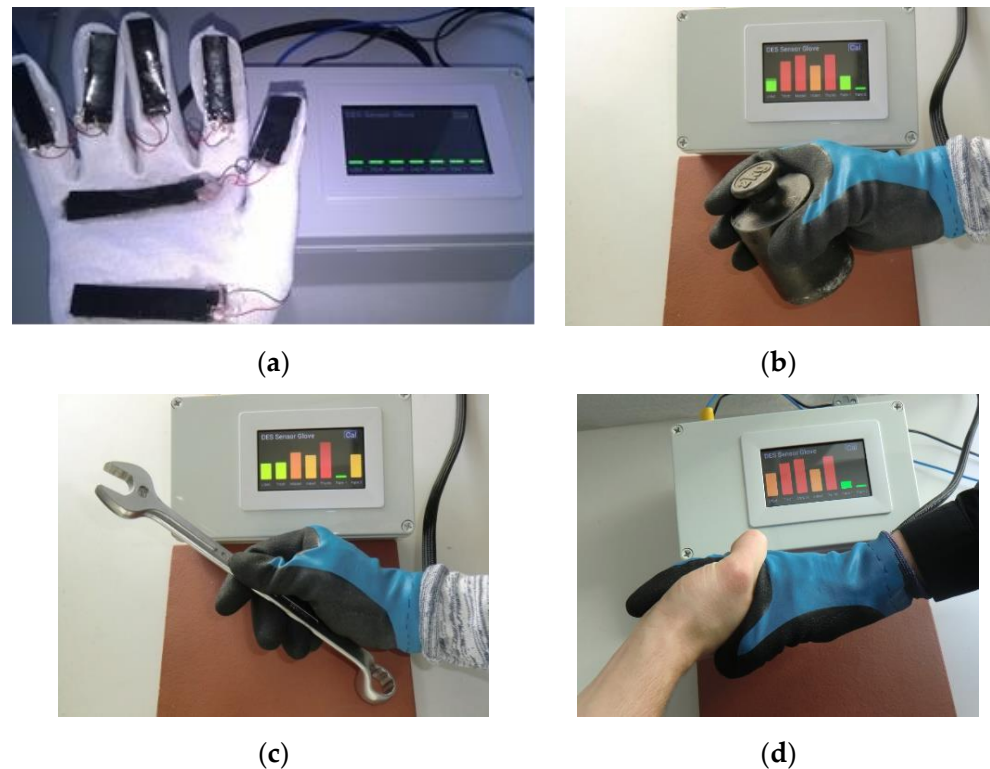


Figure 20. Glove equipped with seven pressure sensors on the fingers and on the palm (a) and sensor signals for different hand operations: grabbing a cylindrical weight (b), grabbing a screw wrench (c) and handshaking (d) [100].

3.2. Human–Machine Interfaces

Beyond the exploitation for monitoring pressure, forces, strain and other deformations, dielectric elastomer sensors with different advanced designs can also be used for human–machine interfaces (HMI) [103]. Here, a human applies a regulated load onto the sensor, which is quantitatively detected and used for the control of a machine or any other device. Some simple examples shall demonstrate this kind of HMI operation.

In Figure 21, a flat panel that contains six pressure sensor fields and six corresponding LEDs is depicted. On this demonstration panel, the pressing force of a finger on any of the six sensor fields triggers the corresponding LED to glow, where the degree of brightness rises with the applied finger force. Additionally, the finger force is also made visible by a green bar on a small display attached to the panel. Figure 21 shows the operation with one finger and the simultaneous operation with two fingers.

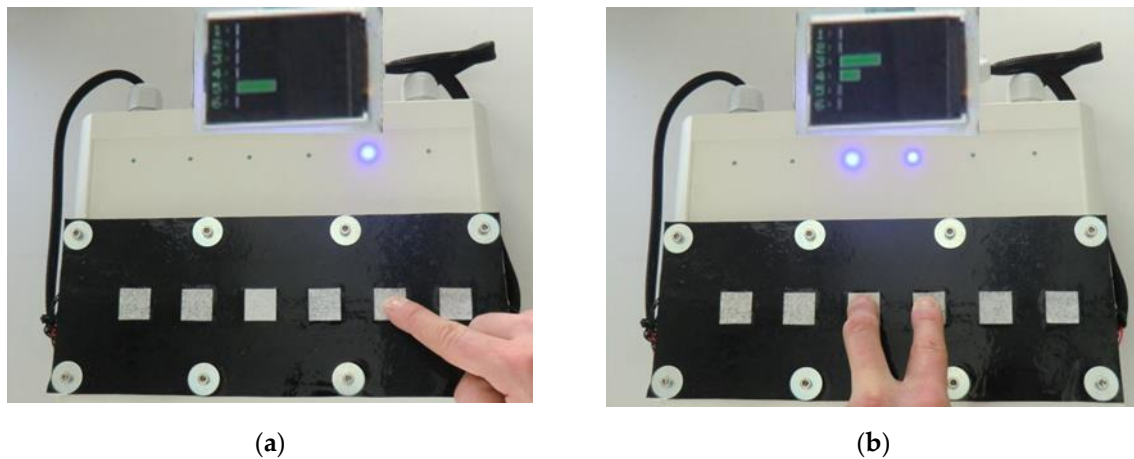


Figure 21. Human–machine interface: a flat panel with six pressure sensors visible as white fields, six corresponding LEDs and a display that illustrates the finger pressure as green bars. Operation with one finger (a) and with two fingers (b) [103].

The same control mechanism with capacitive elastomer sensors can also be transferred to curved surfaces due to the high flexibility of the DES. Figure 22 reveals the integration of four pressure sensors into an automotive steering wheel. The sensors are located below the leather cover on the steering wheel and therefore are not visible. With this control interface, the driver could continuously operate various functions in the car, such as the brightness of a light source, the loudness of a speaker, the ambient temperature or the strength of the air condition. As an example, an increase in pressure enhances the temperature, while a decrease in the pressure reduces it.

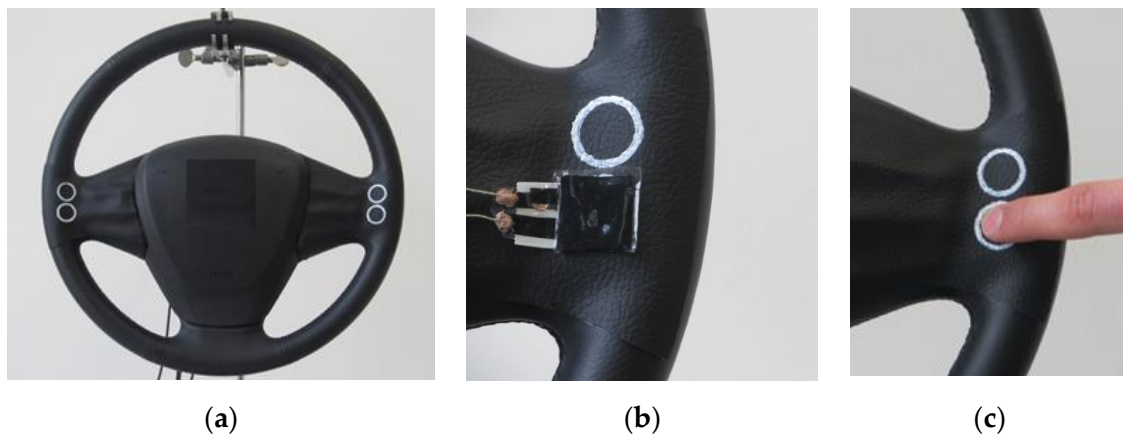


Figure 22. Control interface with four pressure sensors integrated into an automotive steering wheel in overview (a), below the opened leather cover (b) and operated with a finger (c) [103].

The next example concerns a more sophisticated soft and flexible HMI [104]. Here, a pressure sensor with knot profiles is used to monitor the finger pressure applied to it as in the scenarios before. However, this pressure sensor is surrounded by an elastomer frame with four electrically conducting zones. The flexible pressure sensor cannot only be compressed perpendicular to its surface, but it can also be sheared into four different directions. This shear deformation closes one of the four possible electrical contacts on the elastomer frame. With this arrangement, four different technical functions could be addressed by selecting the direction of shearing the sensor and setting it to the intended adjustment by the strength of the finger force on the pressure sensor. The selected adjustment may be fixed with a shear motion in the same direction as before to close the corresponding electrical contact again. This working mechanism is demonstrated with the simple, small

and compact elastomer-based operating device depicted in Figure 23. With this device, the brightness of four LEDs with different colors is consecutively adjusted and held on the selected light intensity as an example.

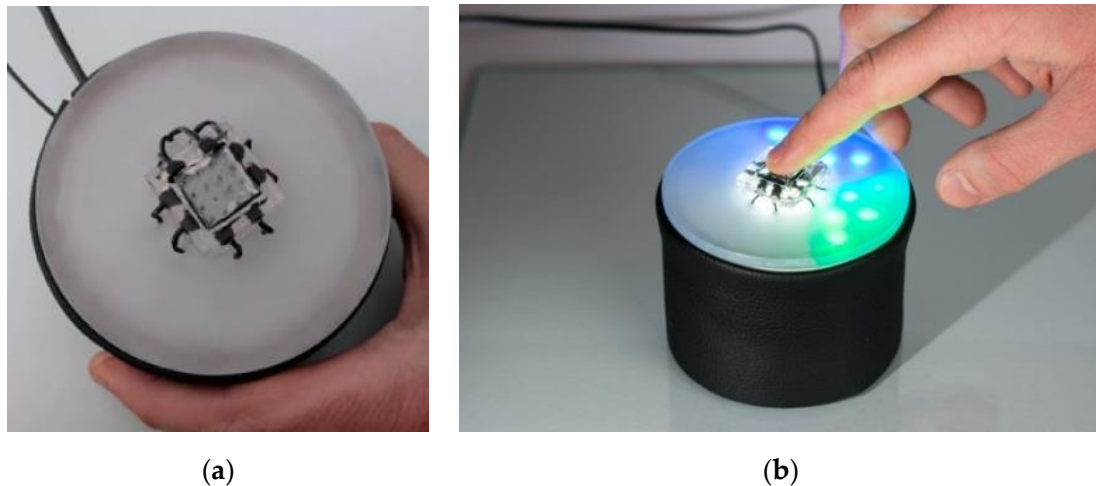


Figure 23. Human-machine interface: a pressure sensor with an elastomer frame containing four electrically conducting zones (a) to close an electrical contact via shear motion of a finger on the pressure sensor, which selects an LED and fixes the tuned brightness of the selected LED (b) [104].

A step forward is the integration of soft capacitive pressure or strain sensors into textiles worn on the human body. A simple demonstrator is shown in Figure 24, which comprises a wristband containing four pressure sensors. By pressing a finger onto one of the pressure sensor fields, the user can continuously control an arbitrary technical function of an electronic device worn on his or her body with the force of the finger. However, the device, which has to be controlled by the wristband, can also be located at a larger distance from the user and thus is operated by a remote control. As depicted in Figure 24d, the strength of the applied pressure on a sensor of the wristband is made visible on a computer display with data transmission via Bluetooth.

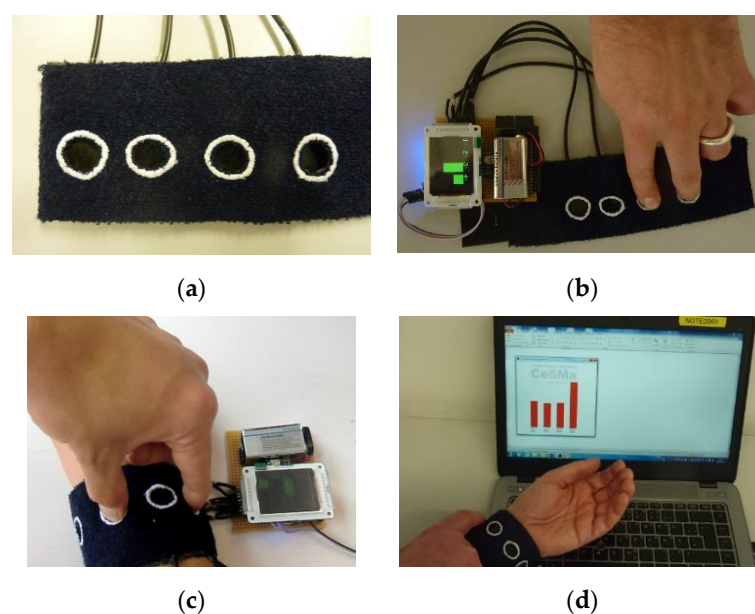


Figure 24. Wristband with four pressure sensors (a) with electronics (b), in operation by a user (c) and with wireless data transfer via Bluetooth to a computer (d) [103].

The most-promising approach with wearable HMI is the realization of an operating glove equipped with various dielectric elastomer sensors. The human hand is able to perform finger motions with high dexterity in multiple degrees of freedom with its five fingers. This enormous versatility can be exploited to conduct complex remote operations if sensors on the glove monitor the finger movements. Special DESs with different functionalities that are integrated into a glove are capable of recording the movements, mutual approaches and pressing forces of the fingers. In the following, some examples of such sensor functionalities are demonstrated.

The first demonstrator is the operating glove shown in Figure 25, which contains three different kinds of DESs [105]:

- Two strain sensors on the backside of the index finger and the middle finger;
- A pressure sensor on the thumb;
- Several contact sensors, which consist of two electrodes located on different fingers.

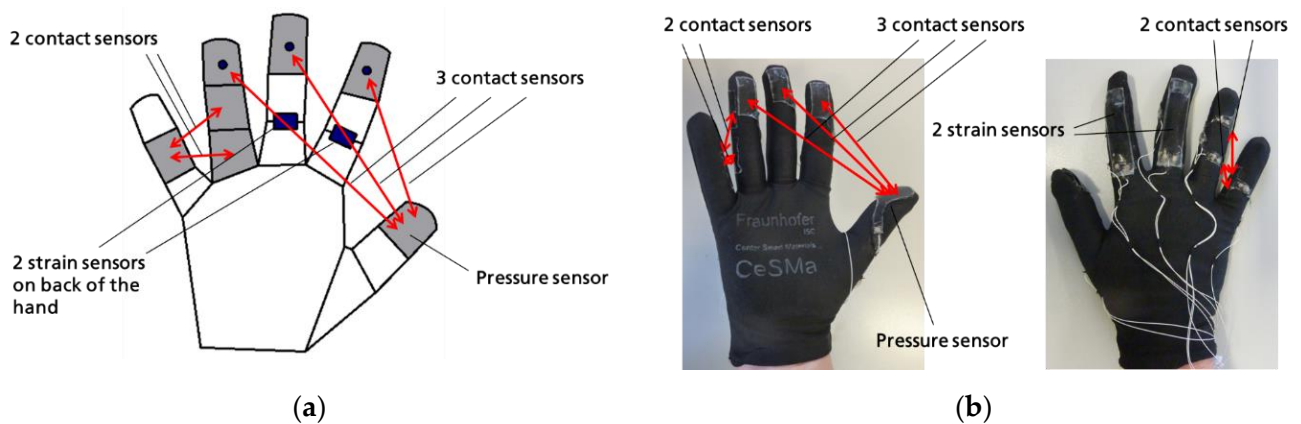


Figure 25. Operating glove with different kinds of DESs. Schematical representation with marked sensor positions (a) and demonstrator of the operating glove with sensors on the front side (left) and on the back side (right) of the hand (b) [105].

The pressure sensor on the thumb measures the force between two fingertips when the thumb is pressed against one of the three consecutive fingers, i.e., index, middle or ring finger. The dosing of the force, which the thumb exerts on the other finger, enables the control of three different technical functions depending on the participating finger (index, middle or ring finger). The selected finger is identified by a contact sensor, which consists of two parts with electrodes distributed over different fingers; one sensor part is located on the thumb, more precisely on the surface of the pressure sensor, and the other sensor part is located on the other finger. When both sensor parts are in contact, where the electrodes are separated only by the dielectric layers on their surfaces, the capacitance between them can be measured. This measurable capacitance between the electrodes located on different fingers identifies their contact.

The structure and the working mechanism of a contact sensor are revealed in Figure 26. When the two fingers approach each other, the two sensor parts with electrodes on the fingers initially have a relatively large distance, which gives a small capacitance between the electrodes. When the distance between the electrodes decreases, the capacitance rises to a maximum when the two sensor parts make contact. In addition to the dielectric layers on the electrodes, which prevent their direct contact, the two sensor parts exhibit another dielectric layer, which insulates the electrode from the humidity of the corresponding finger. Figure 26 also depicts the calculated capacitance per square centimeter, depending on the distance between the sensor parts. This type of sensor works like a proximity sensor but with another electrode configuration than the known proximity sensors.

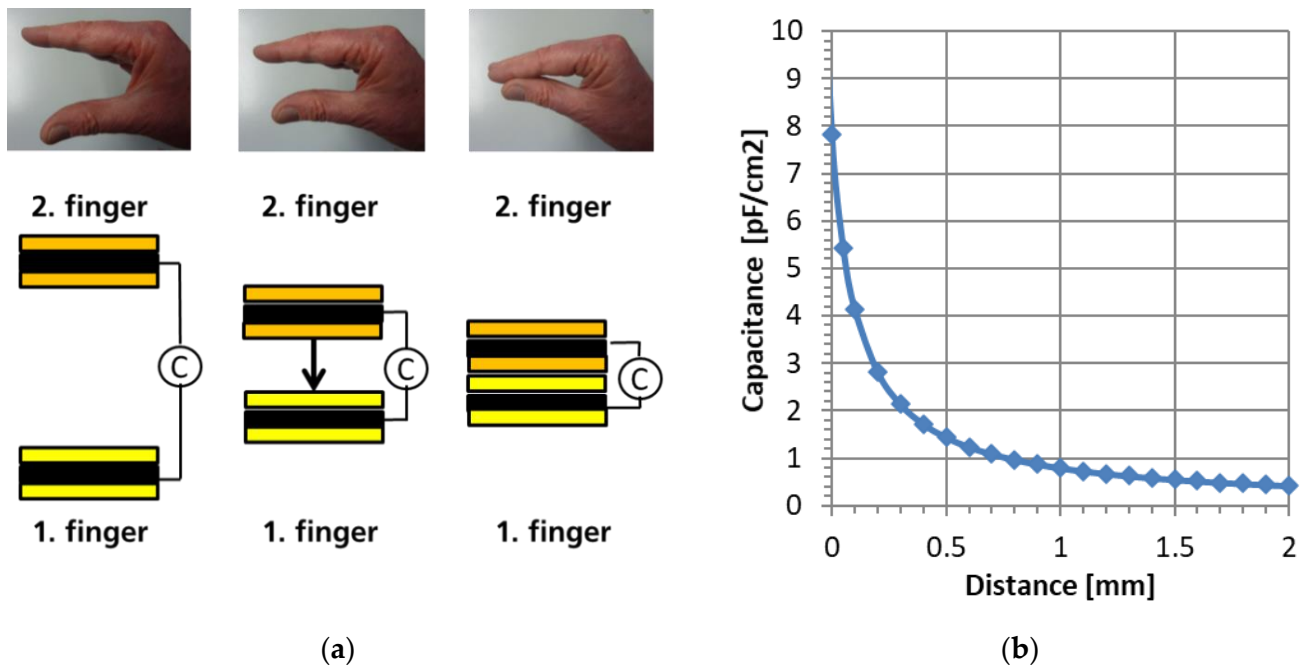


Figure 26. Working mechanism of a contact sensor with two sensor parts with electrodes generating a capacitor distributed over two fingers of a hand, which approach each other (a) and calculated dependence of the capacitance on the distance between the two sensor parts (b) [106].

After identifying the finger that the thumb is in contact with, the strength of the contact force due to the pressing of the two fingers against each other is detected by the pressure sensor on the thumb. The detected degree of pressure can be used to set an intended value of an arbitrary technical function to be controlled by the operating glove. After setting the intended value, another contact sensor on the glove can fix the value and finish this operation. On the operating glove described here, a double contact sensor containing one sensor part with an electrode on the little finger and two sensor parts with electrodes on the ring finger neighboring each other fulfill this operation, where the sensor part on the little finger slides over the two sensor parts on the ring finger with a suitable finger movement.

Corresponding operations may be performed with the strain sensors on the back side of the index and the middle finger. These sensors are operated by bending the finger, which stretches the strain sensor and increases its capacitance. The bending angle of the finger and the corresponding strain of the sensor determine the selected value of the technical function to be tuned. This feature of strain sensors to monitor the bending of a finger was also reported by other authors [65].

In conclusion, this operating glove comprises three different mechanisms of dielectric elastomer sensors. With its strain, pressure and contact sensors, the glove can monitor various finger motions and yield corresponding capacitance signals to control arbitrary technical functions of a remote device.

A second demonstrator of an operating glove is also equipped with additional types of dielectric elastomer sensors, which are named sliding or shear sensors [106]. In order to avoid any confusion, it should be noted that this sensor type is different from the commonly known shear sensors, which measure a shear force or a shear deformation on a surface. Here, two separated parallel surfaces slide along each other to determine the relative position of the surfaces with respect to each other. One of the two surfaces exhibits two neighbored electrode areas covered by dielectric layers on both sides. The other surface carries only one electrode area, which is also covered by dielectric layers on both sides. These two surfaces are located on two different fingers of the glove. When the surface with the two electrodes is in contact with the surface with one electrode, two individual capacitances can be measured between the two electrodes on the first finger

and the counter-electrode on the second finger. Sliding or shearing the second finger over the first finger along the two electrode areas changes both capacitances, where one capacitance becomes larger, and the other one becomes smaller. With these two capacitance values, the position of the second finger on the first finger can be determined. By continuously monitoring the position of the second finger on the first finger, the actual position can be used to control a technical function in a similar way as with strain or pressure sensors. Figure 27 depicts the working mechanism of the sliding or shear sensor schematically.

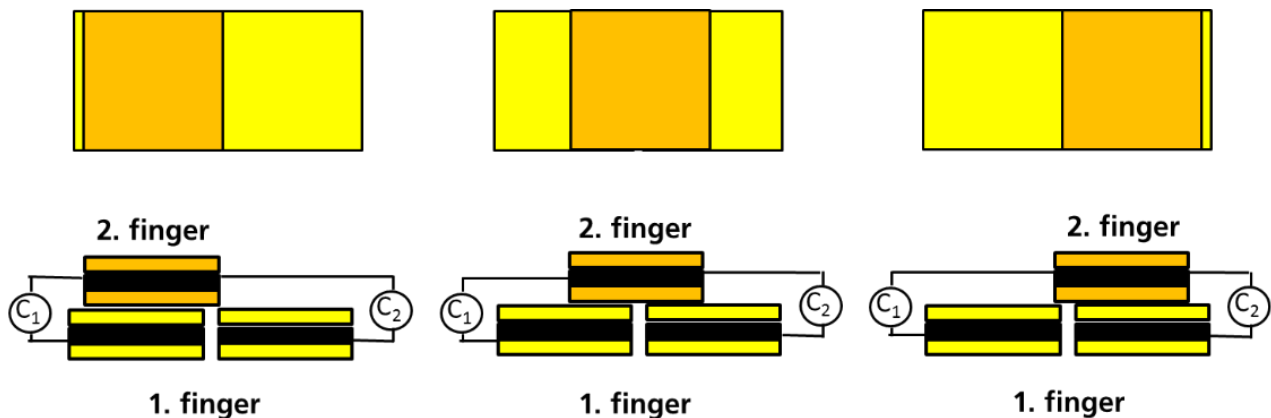


Figure 27. Schematic representation of the working mechanism of a sliding or shear sensor with two electrodes with dielectric layers on one finger and one electrode with dielectric layers on another finger of a hand in top view (**top**) and side view (**bottom**) [106].

With this shear sensor, the sliding movement of the second on the first finger occurs in one dimension. However, this sensor concept can also be extended to two dimensions. For this purpose, the surface of the first finger exhibits four electrode areas covered by dielectric layers, and the second finger carries the counter-electrode with dielectric layers. This arrangement gives four individual capacitors whose capacitances can be continuously monitored. Now, the second finger slides in two dimensions over the first finger, and the positions in both dimensions are determined. The working mechanism of this 2D sliding or shear sensor is depicted in Figure 28. With the 2D position tracking, the sensor has a similar functionality to a computer mouse. The second finger moves a cursor in the x and y dimension. For both the 1D and 2D sliding sensors, the last position of the second on the first finger can be frozen by simply removing the second from the first finger. The removal of the second finger causes all capacitances to become zero as an indicator that the last measured position of the second finger gives the selected setting of the controlled technical function.

Figure 29 shows a schematic of the operating glove equipped with various sliding or shear sensors besides other DESs. The glove exhibits two 1D sliding or shear sensors, where two neighbored electrode areas of each sensor are located on the middle finger and the ring finger, respectively, and the common counter-electrode for both electrode pairs is attached to the thumb. The four neighbored electrode areas of an additional 2D sliding sensor are located on the index finger, and the counter-electrode on the thumb is the same as for the two 1D sliding sensors.

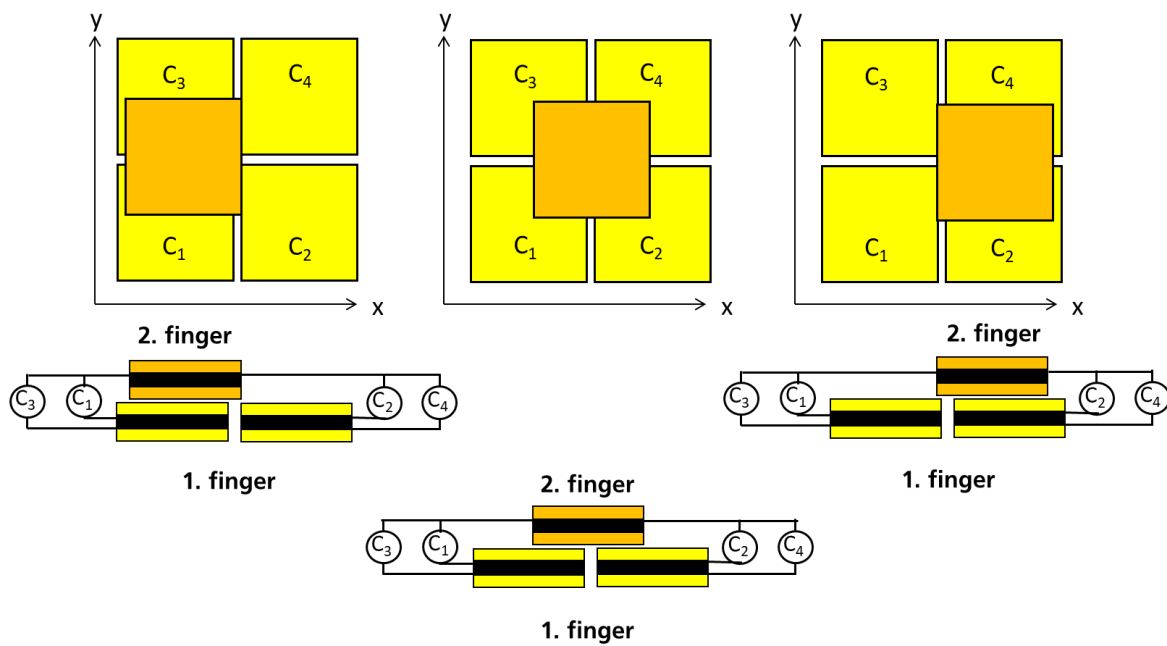


Figure 28. Schematic representation of the working mechanism of a 2D sliding or shear sensor with four electrodes with dielectric layers on one finger and one electrode with dielectric layers on another finger of a hand in top view (**top**) and side view (**bottom**), where the electrodes with dielectric layers, which contribute to the capacitances C_3 and C_4 are not visible in the side view [106].

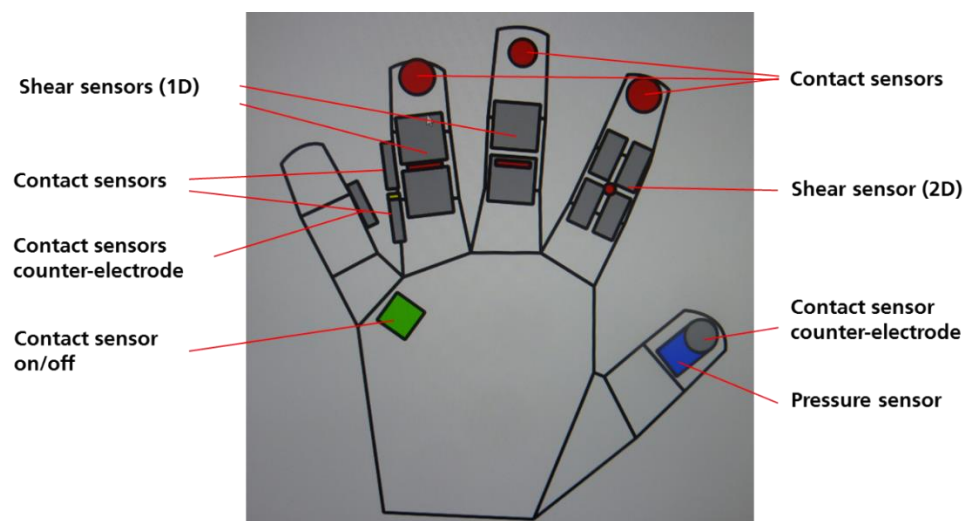


Figure 29. Schematic representation of an operating glove with two 1D and one 2D sliding or shear sensors, a pressure sensor and several contact sensors [106].

Similarly to the former operating glove described before, this glove also exhibits a pressure sensor on the thumb below the counter-electrode and various contact sensors on the tips of the index, middle and ring fingers, which indicate the kind of operation to be controlled by the pressure sensor. An additional contact sensor with one electrode on the palm and the same counter-electrode on the thumb is used as the on/off switch of the operating glove. Finally, two electrodes on the ring finger with the counter-electrode on the little finger serve as another pair of contact sensors for detecting a sliding motion of the little finger along the ring finger in order to freeze the actual value of the pressure sensor. All electrode locations on this operating glove are revealed in the schematical representation in Figure 29.

Figure 30 depicts the demonstration of the operating glove in two stages. The left picture shows the electrodes on the various fingers of the glove, two sets of two electrodes each as parts of the 1D sliding sensors on the middle finger and on the ring finger and a set of four electrodes as part of the 2D sliding sensor on the index finger. Various contact sensors with single electrodes are visible near the tips of the index, middle and ring fingers, where the common counter-electrode for the sliding and the contact sensors is attached to the pressure sensor on the thumb.

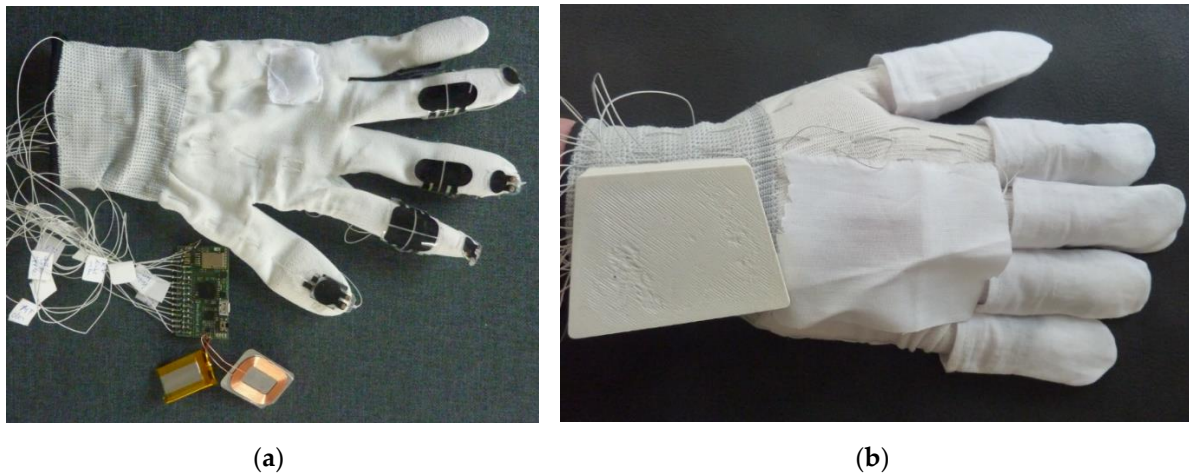


Figure 30. Operating gloves in a disassembled stage with visible sensors, two 1D and one 2D sliding sensors, a pressure sensor, several contact sensors and electronic components (a) and in the final stage with the electronic compartment on the wrist (b) [106].

In the right picture in Figure 30, all electrodes are covered by an additional fabric layer, which also serves as a dielectric layer. Electrical connection lines are guided from all sensor electrodes to the back side of the hand. Here, the operating glove carries a flat electronic compartment containing the microprocessor and other electronic components on a printed circuit board (PCB).

4. Conclusions

Dielectric elastomer sensors as soft, flexible and stretchable material composites exhibit enormous capabilities for the measurement and monitoring of mechanical quantities such as forces and deformations. It was demonstrated that the DES technology goes far beyond the commonly known strain sensors. With suitable designs of the sensors using special dielectric and electrode components, a large variety of DESs with different measuring characteristics can be realized. These characteristics especially concern the dependence of the capacitance increase on the stretch or compression deformation as well as on the applied force or pressure, which allows the tuning of the measuring sensitivity by the sensor design.

This extremely versatile sensor technology opens the way to a wide range of possible applications. DESs are especially useful for wearables to measure the pressure on or the movement of body parts. Furthermore, different types of DESs also offer a very promising potential for human–machine interfaces, where with the application of forces on a sensor and with movements of sensor-equipped fingers, arbitrary technical functions can be remotely controlled. These versatile capabilities give DESs a high potential for a multitude of future applications. It is expected that the first products based on the described sensor technologies could enter the market within the next years.

Author Contributions: Conceptualization, H.B.; methodology, H.B.; validation, H.B. and J.E.; investigation, H.B. and J.E.; writing—original draft preparation, H.B.; writing—review and editing, J.E.; visualization, H.B. All authors have read and agreed to the published version of the manuscript.

Funding: This research was supported by the Bavarian Ministry of Economic Affairs, Regional Development and Energy with funding for the projects ZeSMa and DiMaWert.

Data Availability Statement: More detailed information to this review can be found in the cited references.

Acknowledgments: Financial support from the Bavarian Ministry of Economic Affairs, Regional Development and Energy for the projects ZeSMa and DiMaWert is gratefully acknowledged. The authors thank Dominik Müller, Jinchao Liu, Thomas Gerlach, Eric Fuß, Philipp Lux, Deniz Ocak, Tatjana Shinkar, Detlev Uhl, Maximilian Thuy, Simon Stier and Stefan Muth for their excellent work.

Conflicts of Interest: The authors declare no conflict of interests.

References

1. Carpi, F.; De Rossi, D.; Kornbluh, R.; Pelrine, R.; Sommer-Larsen, P. (Eds.) *Dielectric Elastomers as Electromechanical Transducers*; Elsevier: Amsterdam, The Netherlands, 2008. [\[CrossRef\]](#)
2. Romasanta, L.J.; Lopez-Manchado, M.A.; Verdejo, A. Increasing the performance of dielectric elastomer actuators: A review from the materials perspective. *Prog. Polym. Sci.* **2015**, *51*, 188–211. [\[CrossRef\]](#)
3. Zhang, J.; Wang, Y.; McCoul, D.; Pei, Q.; Chen, H. Viscoelastic creep elimination in dielectric elastomer actuation by preprogrammed voltage. *Appl. Phys. Lett.* **2014**, *105*, 212904. [\[CrossRef\]](#)
4. Madsen, F.B.; Daugaard, A.E.; Hvilsted, S.; Skov, A.L. The Current State of Silicone-Based Dielectric Elastomer Transducers. *Macromol. Rapid Commun.* **2016**, *37*, 378–413. [\[CrossRef\]](#) [\[PubMed\]](#)
5. Böse, H.; Uhl, D.; Flittner, K.; Schlaak, H. Dielectric Elastomer Actuator with Enhanced Permittivity and Strain. *Proc. SPIE* **2011**, *7976*, 734–746.
6. Kussmaul, B.; Risse, S.; Kofod, G.; Waché, R.; Wegener, M.; McCarthy, D.N.; Krüger, H.; Gerhard, R. Enhancement of dielectric permittivity and electromechanical response in silicone elastomers: Molecular grafting of organic dipoles to the macromolecular network. *Adv. Funct. Mater.* **2011**, *21*, 4589–4594. [\[CrossRef\]](#)
7. Böse, H.; Uhl, D.; Rabindranath, R. Novel DEA with organically modified silicone elastomer for permittivity enhancement. *Proc. SPIE* **2012**, *8340*, 538–547.
8. Sheima, Y.; von Szczepanski, J.; Danner, P.; Owusu, F.; Iacob, M.; Perju, E.; Nüesch, F.; Opris, D.M. High dielectric permittivity elastomers: Synthesis, processability, and device manufacturing. *Proc. SPIE* **2022**, *XXIV*, PC120420Q.
9. Shigemune, H.; Sugano, S.; Nishitani, J.; Yamauchi, M.; Hosoya, N.; Hashimoto, S.; Maeda, S. Dielectric Elastomer Actuators with Carbon Nanotube Electrodes Painted with a Soft Brush. *Actuators* **2018**, *7*, 51. [\[CrossRef\]](#)
10. Böse, H.; Uhl, D. Dielectric elastomers with novel highly-conducting electrodes. *Proc. SPIE* **2013**, *8687*, 720–731.
11. Pelrine, R.; Kornbluh, R.; Pei, Q.; Joseph, J. High-speed electrically actuated elastomers with over 100% strain. *Science* **2000**, *287*, 836–839. [\[CrossRef\]](#)
12. Pelrine, R.; Kornbluh, R.; Joseph, J.; Heydt, R.; Pei, Q.; Chiba, S. High-field deformation of elastomeric dielectrics for actuators. *Mater. Sci. Eng. C* **2000**, *11*, 89–100. [\[CrossRef\]](#)
13. O'Halloran, A.; O'Malley, F.; McHugh, P. A review on dielectric elastomer actuators, technology, applications, and challenges. *J. Appl. Phys.* **2008**, *104*, 071101. [\[CrossRef\]](#)
14. Kovacs, G.; Düring, L.; Michel, S.; Terrasi, G. Stacked dielectric elastomer actuator for tensile force transmission. *Sens. Actuators A* **2009**, *155*, 299–307. [\[CrossRef\]](#)
15. Kofod, G. The static actuation of dielectric elastomer actuators: How does pre-stretch improve actuation? *J. Phys. D Appl. Phys.* **2008**, *41*, 215405. [\[CrossRef\]](#)
16. Bruch, D.; Willian, T.P.; Schäfer, H.C.; Motzki, P. Performance-Optimized Dielectric Elastomer Actuator System with Scalable Scissor Linkage Transmission. *Actuators* **2022**, *11*, 160. [\[CrossRef\]](#)
17. Flittner, K.; Schlosser, M.; Schlaak, H.F. Dielectric elastomer stack actuators for integrated gas valves. *Proc. SPIE* **2011**, *7976*, 443–449.
18. Giousouf, M.; Kovacs, G. Dielectric elastomer actuators used for pneumatic valve technology. *Smart Mater. Struct.* **2013**, *22*, 104010. [\[CrossRef\]](#)
19. Linnebach, P.; Rizzello, G.; Seelecke, S. Design and validation of a dielectric elastomer membrane actuator driven pneumatic pump. *Smart Mater. Struct.* **2020**, *29*, 075021. [\[CrossRef\]](#)
20. Heydt, R.P.; Kornbluh, R.; Eckerle, J.; Pelrine, R. *Dielectric Elastomer Loudspeakers*, [*Dielectric Elastomers as Electromechanical Transducers*]; Carpi, F., De Rossi, D., Kornbluh, R., Pelrine, R., Sommer-Larsen, P., Eds.; Elsevier: Amsterdam, The Netherlands, 2008; pp. 313–320.
21. Carpi, F.; Frediani, G.; Turco, S.; De Rossi, D. Bioinspired Tunable Lens with Muscle-Like Electroactive Elastomers. *Adv. Funct. Mater.* **2011**, *21*, 4152–4158. [\[CrossRef\]](#)

22. Shian, S.; Diebold, R.M.; Clarke, D.R. Tunable lenses using transparent dielectric elastomer actuators. *Opt. Express* **2013**, *21*, 8669–8676. [[CrossRef](#)]
23. Giger, J.; Blum, M.; Aschwanden, M. Laser speckle reduction based on electroactive polymers. In Proceedings of the 1st Advanced Laser and Photon Sources (ALPS'12), Yokohama, Japan, 26–27 April 2012.
24. Shintake, J.; Rosset, S.; Schubert, B.; Floreano, D.; Shea, H. Versatile soft grippers with intrinsic electroadhesion based on multifunctional polymer actuators. *Adv. Mater.* **2016**, *28*, 231–238. [[CrossRef](#)] [[PubMed](#)]
25. Guo, Y.; Liu, L.; Liu, Y.; Leng, J. Review of Dielectric Elastomer Actuators and Their Applications in Soft Robots. *Adv. Intell. Syst.* **2021**, *3*, 2000282. [[CrossRef](#)]
26. Matysek, M.; Lotz, P.; Schlaak, H.F. Braille display with dielectric polymer actuator. In Proceedings of the 10th International Conference on New Actuators, Bremen, Germany, 14–16 June 2006; pp. 997–1000.
27. Di, K.; Bao, K.; Chen, H.; Xie, X.; Tan, J.; Shao, X.; Li, Y.; Xia, W.; Xu, Z.; E, S. Dielectric Elastomer Generator for Electromechanical Energy Conversion: A Mini Review. *Sustainability* **2021**, *13*, 9881. [[CrossRef](#)]
28. Koh, A.; Keplinger, C.; Li, T.; Bauer, S.; Suo, Z. Dielectric elastomer generators: How much energy can be converted? *IEEE/ASME Trans. Mechatron.* **2011**, *16*, 33–41. [[CrossRef](#)]
29. Chiba, S.; Waki, M.; Kornbluh, R.; Pelrine, R. Current status and future prospects of power generators using dielectric elastomers. *Smart Mater. Struct.* **2011**, *20*, 124006. [[CrossRef](#)]
30. McKay, T.G.; Rosset, S.; Anderson, I.A.; Shea, H. Dielectric elastomer generators that stack up. *Smart Mater. Struct.* **2015**, *24*, 015014. [[CrossRef](#)]
31. Vertechy, R.; Montana, M.; Rosati Papini, G.P.; Forehand, D. In-tank tests of a dielectric elastomer generator for wave energy harvesting. *Proc. SPIE* **2014**, *9056*, 332–342.
32. Kornbluh, R.; Pelrine, R.; Prahlad, H.; Wong-Foy, A.; McCoy, B.; Kim, S.; Eckerly, J.; Low, T. From boots to buoys: Promises and challenges of dielectric elastomer energy harvesting. *Proc. SPIE* **2011**, *7976*, 67–93.
33. Son, S.; Goulbourne, N.C. Finite Deformations of Tubular Dielectric Elastomer Sensors. *J. Intell. Mat. Syst. Struct.* **2009**, *20*, 2187–2199. [[CrossRef](#)]
34. Xu, D.; McKay, T.G.; Michel, S.; Anderson, I.A. Enabling large scale capacitive sensing for dielectric elastomers. *Proc. SPIE* **2014**, *9056*, 269–276.
35. Rosenthal, M.; Bonwit, N.; Duncheon, C.; Heim, J. Applications of dielectric elastomer EPAM sensors. *Proc. SPIE* **2007**, *6524*, 410–416.
36. Ni, N.; Zhang, L. *Dielectric Elastomer Sensors*; IntechOpen: London, UK, 2017. [[CrossRef](#)]
37. Bae, J.-H.; Chang, S.-H. PVDF-based ferroelectric polymers and dielectric elastomers for sensor and actuator applications: A review. *Funct. Compos. Struct.* **2019**, *1*, 012003. [[CrossRef](#)]
38. Zhao, Y.; Yin, L.-J.; Zhong, S.-L.; Zha, J.-W.; Dang, Z.-M. Review of dielectric elastomers for actuators, generators and sensors. *IET Nanodielectr.* **2020**, *3*, 99–106. [[CrossRef](#)]
39. Rizzello, G. A Review of Cooperative Actuator and Sensor Systems Based on Dielectric Elastomer Transducers. *Actuators* **2023**, *12*, 46. [[CrossRef](#)]
40. Hoffstadt, T.; Griese, M.; Maas, J. Identification of the mechanical state of DEAP transducers based on integrated DEAP sensors. *Proc. SPIE* **2014**, *9056*, 277–288.
41. Gisby, T.A.; O'Brien, B.M.; Anderson, I.A. Self sensing feedback for dielectric elastomer actuators. *Appl. Phys. Lett.* **2013**, *102*, 193703. [[CrossRef](#)]
42. Rizzello, G.; Naso, D.; York, A.; Seelecke, S. Closed loop control of dielectric elastomer actuators based on self-sensing displacement feedback. *Smart Mater. Struct.* **2016**, *25*, 035034. [[CrossRef](#)]
43. Jung, K.; Kim, K.J.; Choi, H.R. A self-sensing dielectric elastomer actuator. *Sens. Actuators A* **2008**, *143*, 343–351. [[CrossRef](#)]
44. Rosset, S.; O'Brien, B.M.; Gisby, T.; Xu, D.; Shea, H.R.; Anderson, I.A. Self-sensing dielectric elastomer actuators in closed-loop operation. *Smart Mater. Struct.* **2013**, *22*, 104018. [[CrossRef](#)]
45. Chuc, N.H.; Thuy, D.V.; Park, J.; Kim, D.; Koo, J.; Lee, Y.; Nam, J.D.; Choi, H.R. A dielectric elastomer actuator with self-sensing capability. *Proc. SPIE* **2008**, *6927*, 260–267.
46. Matysek, M.; Haus, H.; Moessinger, H.; Brokken, D.; Lotz, P.; Schlaak, H.F. Combined Driving and Sensing Circuitry for Dielectric Elastomer Actuators in mobile applications. *Proc. SPIE* **2011**, *7976*, 314–324.
47. Gisby, T.; Xie, S.; Calius, E.; Anderson, I. Integrated sensing and actuation of muscle-like actuators. *Proc. SPIE* **2009**, *7287*, 72–83.
48. Ye, Z.; Chen, Z. Self-sensing of dielectric elastomer actuator enhanced by artificial neural network. *Smart Mater. Struct.* **2017**, *26*, 095056. [[CrossRef](#)]
49. Rizzello, G.; Naso, D.; York, A.; Seelecke, S. A Self-Sensing Approach for Dielectric Elastomer Actuators Based on Online Estimation Algorithms. *IEEE/ASME Trans. Mechatron.* **2017**, *22*, 728–738. [[CrossRef](#)]
50. Rizzello, G.; Fugaro, F.; Naso, D.; Seelecke, S. Simultaneous Self-Sensing of Displacement and Force for Soft Dielectric Elastomer Actuators. *IEEE Robot. Autom. Lett.* **2018**, *3*, 1230–1236. [[CrossRef](#)]
51. Rizzello, G.; Serafino, P.; Naso, D.; Seelecke, S. Towards Sensorless Soft Robotics: Self-Sensing Stiffness Control of Dielectric Elastomer Actuators. *IEEE Trans. Robot.* **2020**, *36*, 174–188. [[CrossRef](#)]
52. Zhang, R.; Irvani, P.; Keogh, P. Closed loop control of force operation in a novel self-sensing dielectric elastomer actuator. *Sens. Actuators A* **2017**, *264*, 123–132. [[CrossRef](#)]

53. Fasolt, B.; Hodgins, M.; Rizzello, G.; Seelecke, S. Effect of screen printing parameters on sensor and actuator performance of dielectric elastomer (DE) membranes. *Sens. Actuators A* **2017**, *265*, 10–19. [[CrossRef](#)]
54. Araromi, O.A.; Rosset, S.; Shea, H.R. High-resolution, large-area fabrication of compliant electrodes via laser ablation for robust, stretchable dielectric elastomer actuators and sensors. *ACS Appl. Mater. Interfaces* **2015**, *7*, 18046–18053. [[CrossRef](#)]
55. Xu, D.; Gisby, T.A.; Xie, S.; Anderson, I.A. Scalable sensing electronics towards a motion capture suit. *Proc. SPIE* **2013**, *8687*, 697–703.
56. O'Brien, B.; Gisby, T.; Anderson, I.A. Stretch sensors for human body motion. *Proc. SPIE* **2014**, *9056*, 254–262.
57. Huang, B.; Li, M.; Mei, T.; McCoul, D.; Qin, S.; Zhao, Z.; Zhao, J. Wearable Stretch Sensors for Motion Measurement of the Wrist Joint Based on Dielectric Elastomers. *Sensors* **2017**, *17*, 2708. [[CrossRef](#)] [[PubMed](#)]
58. Walker, C.; Anderson, I. Monitoring diver kinematics with dielectric elastomer sensors. *Proc. SPIE* **2017**, *10163*, 11–21.
59. Walker, C.; Anderson, I. From land to water: Bringing dielectric elastomer sensing to the underwater realm. *Proc. SPIE* **2016**, *9798*, 443–450.
60. Larson, C.; Spjut, J.; Knepper, R.; Shepherd, R. A Deformable Interface for Human Touch Recognition using Stretchable Carbon Nanotube Dielectric Elastomer Sensors and Deep Neural Networks. *Soft Robot.* **2019**, *6*, 611–620. [[CrossRef](#)]
61. Xu, D.; Tairyach, A.; Anderson, I.A. Where the Rubber Meets the Hand: Unlocking the Sensing Potential of Dielectric Elastomers. *J. Polym. Sci. Part B Polym. Phys.* **2016**, *54*, 465–472. [[CrossRef](#)]
62. Available online: <http://www.stretchsense.com> (accessed on 7 March 2023).
63. Available online: <https://leaptechnology.com> (accessed on 7 March 2023).
64. Available online: <https://promo.parker.com/promotionsite/flexsense/us/en/home> (accessed on 7 March 2023).
65. Orbaugh Antillon, D.W.; Walker, C.; Rosset, S.; Anderson, I.A. The challenges of hand gesture recognition using dielectric elastomer sensors. *Proc. SPIE* **2020**, *11375*, 231–241.
66. Orbaugh, D.; Walker, C.; Rosset, S.; Anderson, I. Jumping into virtual reality with dielectric elastomer sensors. *Proc. SPIE* **2021**, *11587*, 17–31.
67. Loew, P.; Rizzello, G.; Seelecke, S. Pressure monitoring inside a polymer tube based on a dielectric elastomer membrane sensor. *Proc. SPIE* **2018**, *10594*, 324–331.
68. Laflamme, S.; Kolloosche, M.; Connor, J.J.; Kofod, G. Soft capacitive sensor for structural health monitoring of large-scale systems. *Struct. Control Health Monit.* **2012**, *19*, 70–81. [[CrossRef](#)]
69. Yan, J.; Downey, A.; Cancelli, A.; Laflamme, S.; Chen, A.; Li, J.; Ubertini, F. Concrete Crack Detection and Monitoring Using a Capacitive Dense Sensor Array. *Sensors* **2019**, *19*, 1843. [[CrossRef](#)] [[PubMed](#)]
70. Son, S.; Goulbourne, N.C. Dynamic response of tubular dielectric elastomer transducers. *Int. J. Solids Struct.* **2010**, *47*, 2672–2679. [[CrossRef](#)]
71. Wang, S.; Kaaya, T.; Chen, Z. Self-sensing of dielectric elastomer tubular actuator with feedback control validation. *Smart Mater. Struct.* **2020**, *29*, 075037. [[CrossRef](#)]
72. Goulbourne, N.; Son, S.; Fox, J. Self-sensing McKibben actuators using dielectric elastomer sensors. *Proc. SPIE* **2007**, *6524*, 295–306.
73. Kanno, R.; Watanabe, S.; Shimizu, K.; Shintake, J. Self-Sensing McKibben Artificial Muscles Embedded with Dielectric Elastomer Sensor. *IEEE Robot. Autom. Lett.* **2021**, *6*, 6274–6280. [[CrossRef](#)]
74. Kofod, G.; Stoyanov, H.; Gerhard, R. Multilayer coaxial fiber dielectric elastomers for actuation and sensing. *Appl. Phys. A* **2011**, *102*, 577–581. [[CrossRef](#)]
75. Girard, A.; Bigué, J.-P.L.; O'Brien, B.M.; Gisby, T.A.; Anderson, I.A.; Plante, J.-S. Soft Two-Degree-of-Freedom Dielectric Elastomer Position Sensor Exhibiting Linear Behavior. *IEEE/ASME Trans. Mechatron.* **2015**, *20*, 105–114. [[CrossRef](#)]
76. Kim, D.; Lee, C.H.; Kim, B.C.; Lee, D.H.; Lee, H.S.; Nguyen, C.T.; Kim, U.K.; Nguyen, T.D.; Moon, H.; Koo, J.C.; et al. Six-axis capacitive force/torque sensor based on dielectric elastomer. *Proc. SPIE* **2013**, *8687*, 688–696.
77. Hu, X.; Yang, F.; Wu, M.; Sui, Y.; Guo, D.; Li, M.; Kang, Z.; Sun, J.; Liu, J. A Super-Stretchable and Highly Sensitive Carbon Nanotube Capacitive Strain Sensor for Wearable Applications and Soft Robotics. *Adv. Mater. Technol.* **2021**, *7*, 2100769. [[CrossRef](#)]
78. Deng, C. High-performance capacitive strain sensors with highly stretchable vertical graphene electrodes. *J. Mater. Chem. C* **2020**, *8*, 5541. [[CrossRef](#)]
79. Dong, T.; Gu, Y.; Liu, T.; Pecht, M. Resistive and capacitive strain sensors based on customized compliant electrode: Comparison and their wearable applications. *Sens. Actuators A Phys.* **2021**, *326*, 112720. [[CrossRef](#)]
80. Tao, Y.-D.; Gu, G.-Y.; Zhu, L.-M. Design and performance testing of a dielectric elastomer strain sensor. *Int. J. Intell. Robot Appl.* **2017**, *1*, 451–458. [[CrossRef](#)]
81. Shintake, J.; Nagai, T.; Ogishima, K. Sensitivity Improvement of Highly Stretchable Capacitive Strain Sensors by Hierarchical Auxetic Structures. *Front. Robot. AI* **2019**, *6*, 127. [[CrossRef](#)] [[PubMed](#)]
82. Liu, H.; Laflamme, S.; Li, J.; Bennett, C.; Collins, W.; Downey, A.; Jo, H. Experimental Validation of Textured Sensing Skin for Fatigue Crack Monitoring. *Proc. SPIE* **2021**, *11591*, 345–351.
83. Zhu, Y.; Tairyach, A. Using a flexible substrate to enhance the sensitivity of dielectric elastomer force sensors. *Sens. Actuators A Phys.* **2021**, *332*, 113167. [[CrossRef](#)]
84. Liu, J.; Mao, G.; Huang, X.; Zou, Z.; Qu, S. Enhanced Compressive Sensing of Dielectric Elastomer Sensor Using a Novel Structure. *J. Appl. Mech.* **2015**, *82*, 101004. [[CrossRef](#)]

85. Yoon, J.I.; Choi, K.S.; Chang, S.P. A novel means of fabricating microporous structures for the dielectric layers of capacitive pressure sensor. *Microelectron. Eng.* **2017**, *179*, 60–66. [[CrossRef](#)]
86. Peng, S.; Chen, S.; Huang, Y.; Pei, S.; Guo, X. High Sensitivity Capacitive Pressure Sensor with Bi-Layer Porous Structure Elastomeric Dielectric Formed by a Facile Solution Based Process. *Sens. Lett.* **2019**, *3*, 2500104. [[CrossRef](#)]
87. Lee, B.-Y.; Kim, J.; Kim, H.; Kim, C.; Lee, S.-D. Low-cost flexible pressure sensor based on dielectric elastomer film with micro-pores. *Sens. Actuators A* **2016**, *240*, 103–109. [[CrossRef](#)]
88. Nie, B.; Geng, J.; Yao, T.; Miao, Y.; Zhang, Y.; Chen, X.; Liu, J. Sensing arbitrary contact forces with a flexible porous dielectric elastomer. *Mater. Horiz.* **2021**, *8*, 962. [[CrossRef](#)]
89. Kwon, D.; Lee, T.-I.; Kim, M.S.; Kim, S.; Kim, T.-S.; Park, I. Porous dielectric elastomer based ultra-sensitive capacitive pressure sensor and its application to wearable sensing device. In Proceedings of the 2015 Transducers—2015 18th International Conference on Solid-State Sensors, Actuators and Microsystems (TRANSDUCERS), Anchorage, AK, USA, 21–25 June 2015; pp. 299–302.
90. Kwon, D.; Lee, T.-Y.; Shim, J.; Ryu, S.; Kim, M.S.; Kim, S.; Kim, T.-S.; Park, I. Highly Sensitive, Flexible, and Wearable Pressure Sensor Based on a Giant Piezocapacitive Effect of Three-Dimensional Microporous Elastomeric Dielectric Layer. *ACS Appl. Mater. Interfaces* **2016**, *8*, 16922–16931. [[CrossRef](#)]
91. Ham, J.; Huh, T.M.; Kim, J.; Kim, J.-O.; Park, S.; Cutkosky, M.R.; Bao, Z. Porous Dielectric Elastomer Based Flexible Multiaxial Tactile Sensor for Dexterous Robotic or Prosthetic Hands. *Adv. Mater. Technol.* **2022**, *8*, 2200903. [[CrossRef](#)]
92. Zhang, H.; Wang, M.Y.; Li, J.; Zhu, J. A soft compressive sensor using dielectric elastomers. *Smart Mater. Struct.* **2016**, *25*, 035045. [[CrossRef](#)]
93. Hao, W.; Guo, J.; Wang, C.; Wang, S.; Shi, C. A Novel Capacitive-Based Flexible Pressure Sensor Based on Stretchable Composite Electrodes and a Dielectric Elastomer with Microstructures. *IEEE Access* **2020**, *8*, 142811. [[CrossRef](#)]
94. Ma, L.; Shuai, X.; Hu, Y.; Liang, X.; Zhu, P.; Sun, R.; Wong, C.-P. A highly sensitive and flexible capacitive pressure sensor based on a micro-arrayed polydimethylsiloxane dielectric layer. *J. Mater. Chem. C* **2018**, *6*, 13232. [[CrossRef](#)]
95. Zhu, Y.; Giffney, T.; Aw, K. A Dielectric Elastomer-Based Multimodal Capacitive Sensor. *Sensors* **2022**, *22*, 622. [[CrossRef](#)]
96. Zhang, H.; Wang, M.Y. Multi-Axis Soft Sensors Based on Dielectric Elastomer. *Soft Robot.* **2016**, *3*, 3–12. [[CrossRef](#)]
97. Böse, H.; Liu, J.; Gerlach, T. Novel dielectric elastomer sensors for the measurement of elevated pressure loads. *Proc. SPIE* **2021**, *11587*, 1158708.
98. Böse, H.; Fuß, E. Novel dielectric elastomer sensors for compression load detection. *Proc. SPIE* **2014**, *9056*, 232–244.
99. Böse, H.; Fuß, E.; Lux, P. Influence of design and material properties on the performance of dielectric elastomer compression sensors. *Proc. SPIE* **2015**, *9430*, 522–533.
100. Böse, H.; Ocak, D.; Ehrlich, J. Applications of pressure-sensitive dielectric elastomer sensors. *Proc. SPIE* **2016**, *9798*, 451–463.
101. Böse, H.; Ehrlich, J.; Gerlach, T.; Shinkar, T.; Uhl, D. Dielectric elastomer strain sensors with enhanced measuring sensitivity. *Proc. SPIE* **2022**, *12042*, 181–193.
102. Böse, H.; Liu, J. Smart elastomer based liquid level sensors with capacitive and resistive measuring principles. *Proc. SPIE* **2020**, *11375*, 62–74.
103. Böse, H.; Müller, D.; Ehrlich, J. Operation tools with dielectric elastomer pressure sensors. *Proc. SPIE* **2017**, *10163*, 32–42.
104. Böse, H.; Ehrlich, J.; Müller, D. Novel Operation Tools with Compression Sensors for Human-Machine Interfaces. In Proceedings of the Sensor 2017, 18th International Conference on Sensors and Measurement Technology, Nuremberg, Germany, 30 May–1 June 2017; pp. 498–503.
105. Böse, H.; Thuy, M.; Stier, S. Wearable operation device with different types of dielectric elastomer sensors. *Proc. SPIE* **2018**, *10594*, 155–166.
106. Böse, H.; Stier, S.; Muth, S. Glove with versatile operation tools based on dielectric elastomer sensors. *Proc. SPIE* **2019**, *10966*, 242–254.

Disclaimer/Publisher’s Note: The statements, opinions and data contained in all publications are solely those of the individual author(s) and contributor(s) and not of MDPI and/or the editor(s). MDPI and/or the editor(s) disclaim responsibility for any injury to people or property resulting from any ideas, methods, instructions or products referred to in the content.